

Phosphasalen Yttrium Complexes: Highly Active and Stereoselective Initiators for Lactide Polymerization

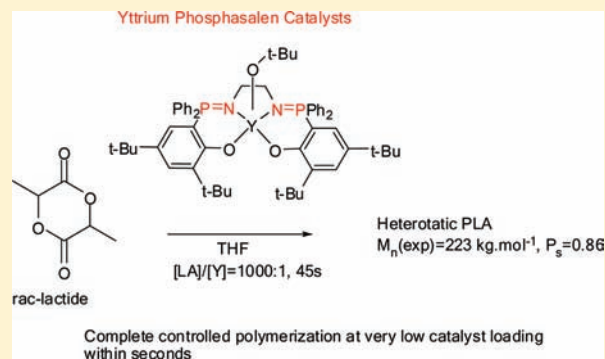
Thi-Phuong-Anh Cao,[†] Antoine Buchard,[‡] Xavier F. Le Goff,[†] Audrey Auffrant,^{*,†} and Charlotte K. Williams^{*,‡}

[†]Laboratoire Hétéroéléments et Coordination, Ecole Polytechnique, CNRS, 91128 Palaiseau Cedex, France

[‡]Department of Chemistry, Imperial College London, London, SW7 2AZ, United Kingdom

S Supporting Information

ABSTRACT: Preparation and characterization of three yttrium alkoxide complexes with new phosphasalen ligands are reported. The phosphasalens are analogues of the well-known salen ligands but with iminophosphorane donors replacing the imine functionality. The three yttrium alkoxide complexes show mono- and dinuclear structures in the solid state, depending on the substituents on the ligand. The new ligands and complexes are characterized using multinuclear NMR spectroscopy, mass spectrometry, elemental analysis, and single-crystal X-ray diffraction experiments. The complexes are all rapid initiators for lactide polymerization; they show excellent polymerization control on addition of exogenous alcohol. The mononuclear complex shows extremely rapid rates and a high degree of stereocontrol in *rac*-lactide polymerization, yielding heterotactic PLA (P_s of 0.9). The phosphasalens are, therefore, excellent ligands for lactide ring-opening polymerization catalysis showing superior rates and stereocontrol versus salen ligands, which may be related to their excellent donating ability and the high degrees of steric protection they can confer.



INTRODUCTION

The tetradentate Schiff base ligand *N,N*-bis(salicylidine)-ethylenediamine or salen is a ubiquitous ancillary ligand in catalysis.¹ Perhaps the most well-known application of this ligand is in the metal-catalyzed asymmetric epoxidation and kinetic resolution of epoxides.^{1a-c} The salen ligand class has also been very successfully applied in polymerization catalysis, for example, in the stereoselective ring-opening polymerization of lactide² and epoxides,³ and copolymerization of epoxides and carbon dioxide.⁴ Optimization of the catalytic activity and selectivity has led to new generations of salen ligands, where changes to the diimine linker, phenol ring substituents, and even reduction of the one/both of the imine groups to amine (so-called salan ligands) has been achieved.^{4a-f} This is a fruitful area for catalysis but also a crowded one. Surprisingly, there have been very few reports of heteroatom substitution on the backbone of the salen ligand.⁵ On the other hand, iminophosphorane moieties are now quite well-established ligands in coordination chemistry and even in catalysis.^{6,7} Iminophosphorane ligands are of interest because, in contrast to imine moieties, they lack π -accepting ability due to the absence of any π system. Therefore, this ligand class behaves as strong σ and π donors due to the presence of two lone pairs on the N atom. Some of us have already reported the preparation of phosphasalen complexes of Ni(II) and Pd(II) which differ from conventional salen complexes in both their electronic and their steric properties.⁸ Motivated by interest in developing new

initiators for ring-opening polymerizations, we prepared several new yttrium alkoxide complexes with the phosphasalen ligand; these complexes are studied for lactide polymerization, where they show superior properties to the salen analogues.

Ring-opening polymerization of lactide (LA) is an interesting process not the least of which is because the product, polylactide (PLA), is a degradable polymer suitable for applications in medicine and as a degradable commodity plastic.⁹ The monomer, lactide, derives from lactic acid which is produced by fermentation of sugars, produced from high starch content plants. Therefore, PLA is widely investigated and commercially produced as a sustainable alternative to petrochemicals. The most efficient synthesis, and the commercial route to PLA, involves ring-opening polymerization of lactide.^{9d,10} This can be accomplished by a wide range of metal complexes, most usually metal alkoxide or amido species, or by organocatalysts and even by enzymes.^{10,11} Application of metal catalysts is attractive as it can lead to high rates, good degrees of polymerization and stereocontrol, and production of block copolymers.^{9d,10a} Selection of the metal catalyst is critical in controlling the properties of PLA. Yttrium and other Group 3 complexes are particularly promising as they exhibit high rates and, through careful selection of the ancillary ligand, can enable stereocontrol.^{2b,12} Yttrium salen complexes were first inves-

Received: September 14, 2011

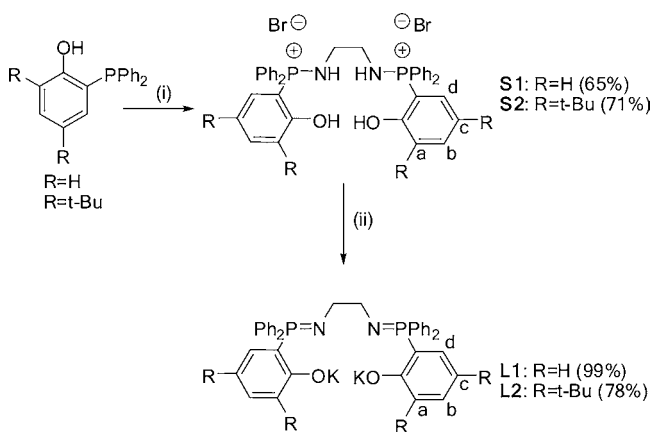
Published: February 7, 2012

tigated nearly a decade ago by Ovitt and Coates; they showed moderate rates but lack polymerization or tacticity control.^{2b,12ad} Carpentier and colleagues also studied alkoxide/phenolate ligands, related to salens, which were slow initiators and produced atactic PLA.^{12q} Recently, Diaconescu and co-workers reported a salen derivative with a ferrocenediyl unit in the imine backbone; it showed faster rates.^{12r} Phenolate–amine ligands have generally proved quite effective; for example, the groups of Carpentier, Mountford, and others have widely investigated application of amino–diphenolate yttrium initiators, which show good/excellent rates and high degrees of stereocontrol.^{12a–h,13} Okuda pioneered the use of dithia–alkanediy-bridged diphenolate Group 3 complexes, some of which showed excellent heteroselectivity via a dynamic monomer recognition process controlled by interconversion of initiator enantiomers.^{12s–u} The complexes also yield highly syndiotactic PLA from *meso*-LA.¹²ⁿ Arnold and co-workers recently reported an interesting initiating system comprising a racemic mixture of alkoxide–phosphine oxide yttrium complexes, which yielded isotactic PLA from *rac*-LA.^{12w,x} Finally, our research group prepared bis(phosphinic/thiophosphinic)-diamido yttrium complexes which show very high rates of polymerization and, in some cases, good heteroselectivity ($P_s = 0.8$).^{12i–m}

RESULTS AND DISCUSSION

Synthesis and Characterization of Yttrium–Phosphasalen Complexes. Our previous lactide polymerization catalyst development work utilized phosphorus-substituted ancillary ligands, in particular, phosphinic amido ligands and iminophosphoranes.^{7,12i–m} These showed high rates for lactide ring-opening polymerization. It was, therefore, of interest to continue to develop this type of ligand and study its catalytic polymerization activity. Given the ubiquity and utility of salen ligands, we were interested in targeting an iminophosphorane analogue (phosphasalen) of this ligand class. Two new phosphasalen ligands were prepared (Scheme 1).

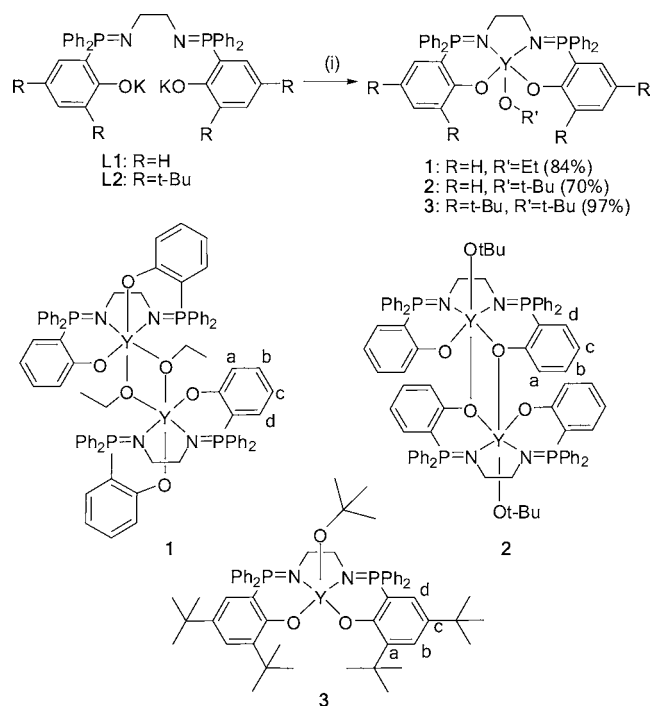
Scheme 1. Synthesis of Phosphasalen Ligands^a



^aReagents and conditions: (i) Br₂ (1 equiv), CH₂Cl₂, 45 min, then ethylenediamine (0.5 equiv), Bu₃N (1 equiv), 16 h; (ii) KHMDS (4 equiv), THF, 298 K, 16 h.

The diphenoldiphosphonium salts S1 and S2 were obtained by a Kirsanov reaction between ethylenediamine and *o*-diphenylphosphinophenol, Scheme 2. They were deprotonated in essentially quantitative yield (except for L2 due to solubility

Scheme 2. Synthesis of Phosphasalen–Yttrium Complexes^a



^aReagents and conditions: (i) [YCl₃(THF)_{3.5}] (1 equiv), THF, 298 K, 1–2 h, then *t*-BuOK (1 equiv) or EtOK (1 equiv), 298 K, 7 h. Labeling schemes of the complexes are used for NMR characterization.

issues) using potassium hexamethyldisilazide. This synthetic strategy is quite useful as it produces high yields of pure product and is compatible with a range of substituents on the phenoxide ring or diamine backbone. Hence, from the related phosphinophenol, the phosphasalen ligands L1 and L2 were obtained, respectively, in 64 and 55% yield overall within two steps.

Reaction of ligand L1 with [YCl₃(THF)_{3.5}] in tetrahydrofuran resulted in immediate precipitation of a white product. The ³¹P{¹H}NMR spectrum showed complete consumption of ligand, as evidenced by the disappearance of the signal at 18.6 ppm. The total insolubility of the product prevented any further analysis; the product is believed to be a cluster/polymer of the ligand–yttrium–chloride. A similar effect has been observed by Diaconescu and co-workers using related yttrium chloride Schiff base complexes.^{5a,12r} Despite the insolubility of the product, addition of an equivalent of potassium *tert*-butoxide/ethoxide into the reaction mixture induced slow dissolution. The ³¹P{¹H}NMR spectrum of the solution presented a single signal at significantly lower field compared to the dianionic ligand, indicating coordination of the phosphasalen ligand to the yttrium center. After removal of the potassium salt, the ethoxide and *tert*-butoxide phosphasalen–yttrium complexes (complexes 1 and 2, respectively) were isolated as white solids, which were characterized by multinuclear NMR spectroscopy, elemental analyses, and single-crystal X-ray diffraction experiments (Table 1).

Both complexes 1 and 2 adopt a dimeric structure in the solid state (Figures 1 and 2 and Tables 2 and 3) with the yttrium centers exhibiting a distorted octahedral geometry formed by the tetradentate phosphasalen ligand, the alkoxide group, and a phenoxide/alkoxide bridge. Both dimers are symmetric: there is no difference between the two yttrium

Table 1. Crystallographic Data for Compounds 1–3

	1	2	3
formula	C ₈₀ H ₇₄ N ₄ O ₆ P ₄ Y ₂ · 2(C ₇ H ₈)	C ₈₄ H ₈₂ N ₄ O ₆ P ₄ Y ₂ · 3(C ₇ H ₈)	C ₅₈ H ₇₃ N ₂ O ₃ P ₂ Y
M _r	1673.40	1821.64	997.03
space group	P-1	P-1	C2/c
T (°C)	−123	−123	−123
λ (Å)	0.71069	0.71069	0.71069
a (Å)	12.950(1)	10.530(1)	20.514(1)
b (Å)	13.948(1)	14.575(1)	27.064(1)
c (Å)	14.744(1)	16.430(1)	22.120(1)
α (deg)	102.175(1)	65.436(1)	90.00
β (deg)	108.382(1)	87.959(1)	117.231(1)
γ (deg)	112.817(1)	89.298(1)	90.00
V (Å ³)	2153.9(3)	2291.9(3)	10919.7(8)
Z	1	1	8
d (g cm ^{−3})	1.290	1.320	1.213
μ (cm ^{−1})	1.469	1.387	1.170
R ₁ ^a	0.0539	0.0562	0.0458
wR ₂ ^b	0.1368	0.1134	0.0813
CCDC no.	836603	836604	836605

$${}^a R_1 = \frac{\sum ||F_o| - |F_c||}{\sum |F_o|}, \quad {}^b wR_2 = \left\{ \frac{\sum [w(F_o^2 - F_c^2)^2]}{\sum [w(F_o^2)]} \right\}^{1/2}; \quad w^{-1} = \sigma^2(F_o^2) + (aP)^2 + bP.$$

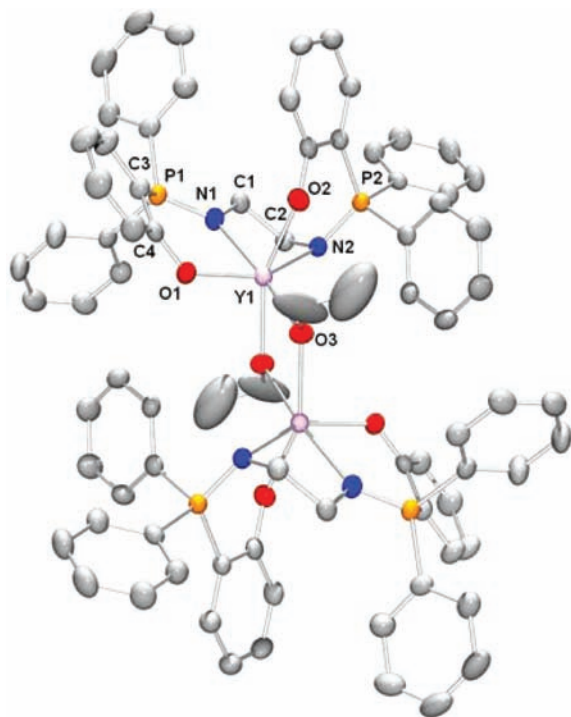


Figure 1. ORTEP view of the solid-state structure of complex 1, with thermal ellipsoids drawn at the 50% probability level. Hydrogen atoms are omitted for clarity.

centers in either complex; thus, all selected bond lengths and angles are represented for only one yttrium center.

In complex 1, the ethoxide groups bridge between the two metal centers, forming a [Y₂O₂] four-membered ring (Figure 1). The ligand adopts a *cis-β*-configuration around the metal: one phenoxide (O2) and one bridging ethoxide group (O3#2) occupy axial coordination sites at the yttrium center. The yttrium center and the other four coordinated atoms (O1, N1, N2, O3) are almost coplanar (dihedral angle (O1, N1, N2, O3) = 1.52(22)°, (Y, N1, O1, O3) = 0.11(25)°). The yttrium–O(phenoxide) (Y–O2) bond, in the axial site, is slightly longer

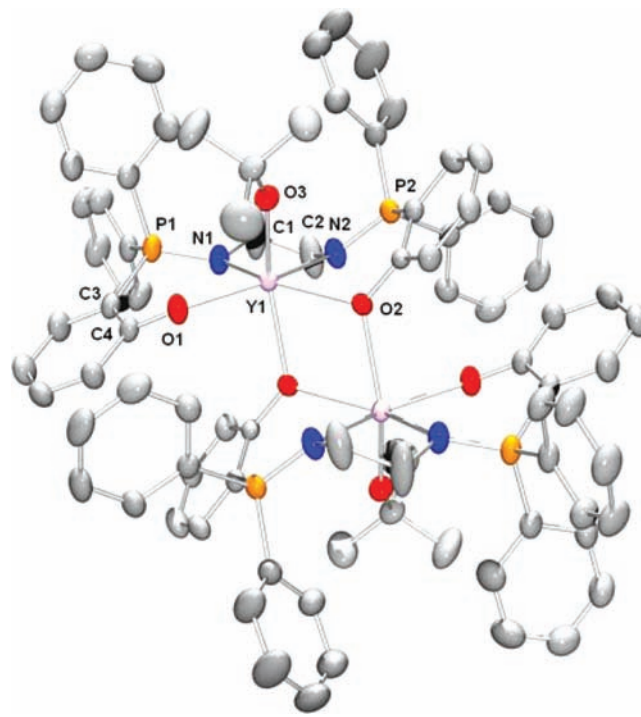


Figure 2. ORTEP view of the solid-state structure of complex 2, with thermal ellipsoids drawn at the 50% probability level. Hydrogen atoms are omitted for clarity.

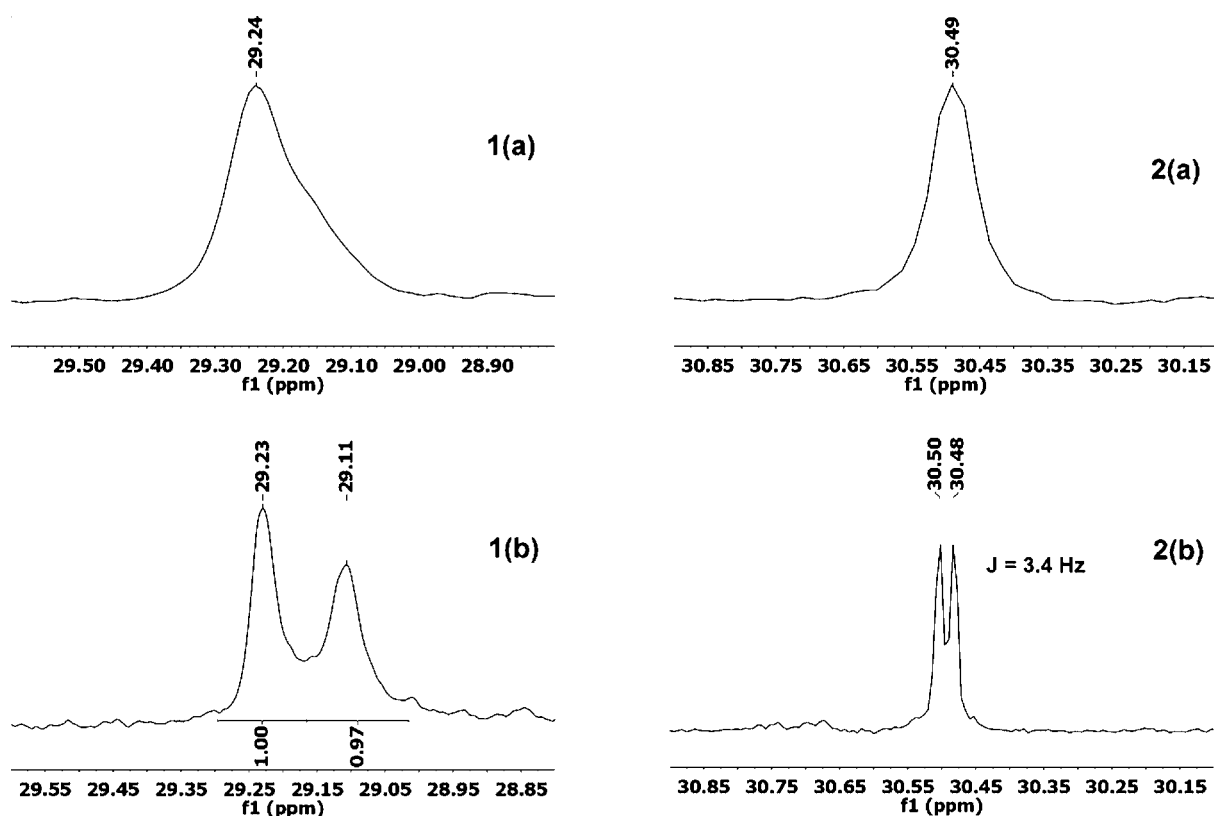
than that in the equatorial position (Y–O1) (2.213(3) vs 2.182(3) Å), whereas the Y–O(ethoxide) (Y–O3#2) bond in the axial position is slightly shorter than that in the equatorial site (Y–O3) (2.243(3) vs 2.273(3) Å). Both yttrium–alkoxide bonds are longer than the yttrium–phenoxide bonds (2.243(3) and 2.273(3) Å vs 2.182(3) and 2.213(3) Å), probably because of their bridging coordination modes. There is almost no difference between the bond lengths of Y–N1 and Y–N2 nor between N1–P1 and N2–P2, respectively. However, the distance Y–P1 is significantly longer than Y–P2 (3.561(1) vs 3.414(1) Å), and the Y–N1–P1 angle is larger than Y–N2–P2

Table 2. Selected Bond Lengths (Angstroms) and Angles (degrees) for Compound 1

Y1–Y1#2	3.6492(7)	Y1–N2	2.438(3)	N2–Y1–O2	81.4(1)
Y1–O1	2.182(3)	P1–N1	1.598(3)	O1–Y1–O2	97.1(1)
Y1–O2	2.213(3)	P2–N2	1.595(3)	O2–Y1–O3	90.6(1)
Y1–O3	2.273(3)	O1–Y1–N1	78.8(1)	O2–Y1–O3#2	156.1(1)
Y1–O3#2	2.243(3)	O2–Y1–N1	90.5(1)	N1–Y1–N2–O2	86.40(11)
Y1–N1	2.415(3)	N1–Y1–N2	70.4(1)	O1–Y1–N2–N1	4.05(25)

Table 3. Selected Bond Lengths (Angstroms) and Angles (degrees) for Compound 2

Y1–O1	2.203(3)	P2–N2	1.586(3)	O2#2–Y1–O3	148.8(1)
Y1–O2	2.338(2)	O1–Y1–N1	78.6(1)	Y1–O2–N2–N1	9.39(24)
Y1–O3	2.079(3)	O2–Y1–N1	143.7(1)	Y1–O1–N1–N2	6.29(26)
Y1–O2#2	2.312(2)	N1–Y1–N2	70.4(1)	O1–N1–Y1–O3	88.49(11)
Y1–N1	2.398(3)	N2–Y1–O2	74.9(1)	O1–N1–Y1–O2#2	82.27(10)
Y1–N2	2.372(3)	O1–Y1–O2	133.0(1)		
P1–N1	1.596(3)	O2–Y1–O3	89.2(1)		

Figure 3. $^{31}\text{P}\{^1\text{H}\}$ NMR spectra of complexes 1 and 2 recorded in THF on (a) 300 and (b) 500 MHz instruments.

($123.81(17)^\circ$ vs $114.05(17)^\circ$). These differences clearly show that the two phosphorus atoms are in slightly different coordination environments, in accordance with them being linked to two phenoxide groups in differing environments (axial vs equatorial positions).

As a consequence, the $^{31}\text{P}\{^1\text{H}\}$ NMR spectrum of complex 1 in THF recorded on a 500 MHz instrument exhibits two signals of equal intensity, very close to each other (Figure 3). These signals are not part of a doublet as they are separated by 25 Hz, which is significantly larger than previously reported $^2J_{\text{YP}}$ coupling constants for similar complexes.^{5a,12i–m,14} When the spectrum was recorded on a lower frequency (300 MHz) instrument, the signals were not resolved and merged into a single broad signal.

Complex 2 is also a dimer in the solid state; however, changing the alkoxide coligand from ethoxide to *tert*-butoxide changes the structure of the complex (Figure 2). The two yttrium centers remain in distorted octahedral geometries, but the *tert*-butoxide ligands now occupy the axial positions, presumably due to steric hindrance preventing them from adopting bridging coordination modes. The complex adopts a trans coordination geometry with a single μ -phenoxide coordination mode per ligand. The Y–N and P–N bond lengths are comparable to those in complex 1, but the Y–O(μ -phenoxide) bond is longer (2.338(2) vs 2.203(3) Å) and the Y–O(alkoxide) bond is significantly shorter (2.079(3) vs 2.243(3) Å). Although the two phenoxide oxygen atoms adopt different coordination modes, the two phosphorus atoms are in almost identical environments, as shown by close similarity in

the P–Y distances (3.490(1) vs 3.507(1) Å) and the P–N–Y bond angles (121.55(18)° vs 122.48(18)°). Indeed, in the $^{31}\text{P}\{^1\text{H}\}$ NMR spectrum of complex 2, in THF, only a single doublet is observed due to coupling with the yttrium center. The value of the coupling constant ($^2J_{\text{YP}} = 3.4$ Hz) is comparable with other reported values for $^2J_{\text{YP}}$ in similar complexes.^{12i–k,m} This provides some indication that the solid-state structure may be maintained in solution.

Complex 3 was prepared from a phosphasalen ligand with sterically hindered *tert*-butyl substituents on the phenoxide ring and with a *tert*-butyl alkoxide coligand (Scheme 2). This ligand was deliberately targeted so as to prevent dimerization and enable isolation of a mononuclear yttrium alkoxide complex. The $^{31}\text{P}\{^1\text{H}\}$ NMR spectrum, in THF, showed a single doublet, at 31.6 ppm, with a coupling constant of 3.0 Hz, suggesting that complex 3 adopts a trans configuration in an analogous manner to complex 2. On examination of the NMR spectra of complexes 2 and 3 some clear differences were observed. In particular, the $^{13}\text{C}\{^1\text{H}\}$ NMR spectra showed that the quaternary phenolate carbon atoms are equivalent in the spectrum of compound 3, whereas they are different in the case of compound 2 (and compound 1), giving rise to two doublets, likely due to the bridging and nonbridging coordination modes of the phenolate. This supported the notion that complex 3 has a mononuclear structure. Definitive evidence concerning the structure of complex 3 was obtained by X-ray diffraction analysis of monocrystals grown from a saturated solution of 3 in cyclohexane (Figure 4 and Table 4). The complex adopts

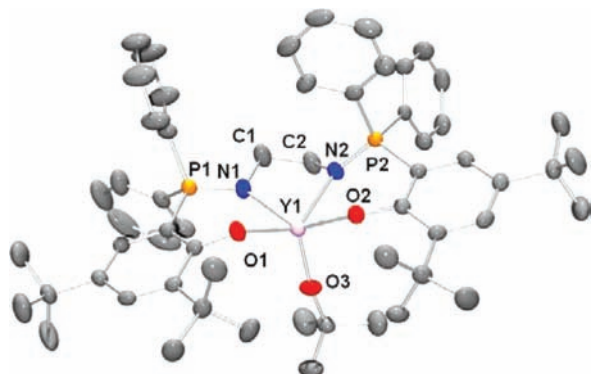


Figure 4. ORTEP view of the solid-state structure of complex 3 with thermal ellipsoids drawn at the 50% probability level. Hydrogen atoms are omitted for clarity.

square-based pyramidal geometry, with the four coordinating atoms of the phosphasalen ligands forming the basal plane, as shown by the dihedral angle O1–N1–N2–O2 (4.13(0.11)°). The yttrium center is slightly out of the medial plane of these four atoms (0.7472 (0.0011) Å). The angle at O3 atom is close to 180°, which probably results from the steric hindrance of the phosphasalen ligand in the basal plane. All yttrium–nitrogen

and yttrium–oxygen bonds in complex 3 are slightly shorter compared to the corresponding values in complexes 1 and 2, probably as a result of the pentacoordination mode.

Lactide Ring-Opening Polymerization. All three complexes were highly active initiators for ring-opening polymerization (ROP) of lactide, Table 5. Selection of the polymerization solvent was critical, with initiator decomposition occurring in methylene chloride and the partial solubility of lactide in toluene (at ambient temperature) leading to heterogeneous polymerization, albeit extremely rapidly. The optimum solvent for use at ambient temperature (25 °C) was THF; all experiments were conducted using an initial concentration of lactide of 1 M, so as to enable accurate comparison between the different initiators and additives.

Initiator 3. Complex 3 is extremely active; it is even able to polymerize unpurified lactide. Near quantitative conversion is reached within 2 min at low initiator loadings ($[\mathbf{3}] = 1$ mM). The polymerization rate was analyzed by taking aliquots; the pseudo-first-order rate constant, k_{obs} , was 0.08 s⁻¹ at $[\mathbf{3}] = 1$ mM (Figure 6). The rate of polymerization is thus among the highest values reported for this reaction, easily comparing with related yttrium systems and outstripping many other metal centers.^{9d,10} Figure 5 and Table 6 compare the polymerization results with other yttrium salen initiators.

Initiator 3 is significantly faster at lower loadings than comparable yttrium salen analogues. Although caution should be applied in comparing values as the experiments were not run under identical conditions, it is clear that initiator 3 shows remarkably enhanced rates, even under significantly lower loadings than literature yttrium complexes, Figure 5. For example, complex 6^{2d} took 14 h to reach complete conversion at 100:1 loading of lactide:initiator, complex 5^{13c} took 1 h to reach complete conversion at a loading of 300:1, and the ferrocenyl salen complex 4^{12r} took 40 min to reach high conversions at a loading of 500:1. In contrast, complex 3 was able to completely polymerize as many as 5000 equiv of lactide in 30 min and 1000 equiv in less than 1 min. It is also notable that initiator 3 can be used at rather low loadings, down to $[\text{LA}]:[\mathbf{3}] = 5000$, which is useful for production of high molecular weight PLA (up to 700 kg/mol). Finally, it is apparent that the other yttrium salen complexes do not allow significant stereocontrol in *rac*-lactide ROP; in contrast, complex 3 enables a high degree of heteroselectivity in *rac*-LA ROP.

The LA ROP using initiator 3 is quite well controlled with the number-averaged molecular weight (M_n) of the PLA increasing linearly with percentage conversion (Figure 7) and polydispersity indices remaining narrow throughout polymerization (<1.4). The experimentally determined values for the number-averaged molecular weight exceed those calculated (on the basis of initiator concentration and conversion). This could be due to either incomplete initiation from the *tert*-butyl alkoxide groups or partial deactivation of the initiator. In order

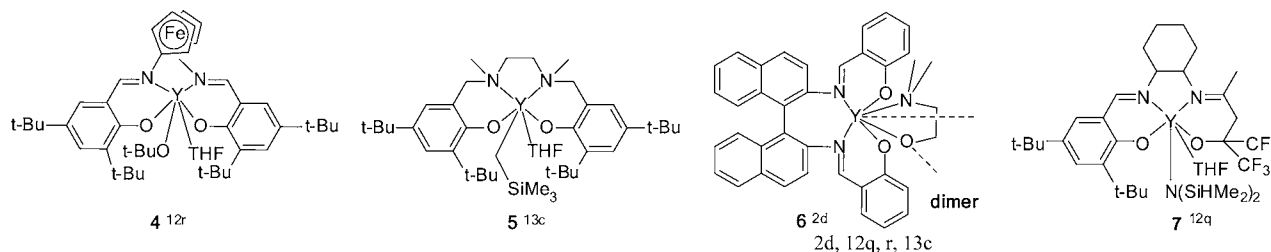
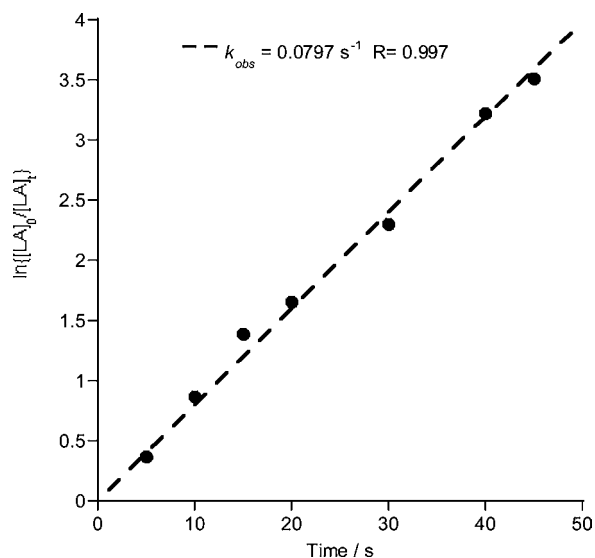
Table 4. Selected Bond Lengths (Angstroms) and Angles (degrees) for Compound 3

Y1–O1	2.1671(318)	P2–N2	1.584(2)	O2–Y1–O3	109.16(8)
Y1–O2	2.1704(18)	O1–Y1–N1	80.51(7)	O1–Y1–O3	115.03(8)
Y1–O3	2.025(2)	O2–Y1–N1	139.87(8)	C55–O3–Y1	171.40 (19)
Y1–N1	2.375(2)	N1–Y1–N2	71.78(8)	O1–N1–N2–O2	4.13(0.11)
Y1–N2	2.324(2)	N2–Y1–O2	79.68(7)	O1–N1–N2–Y1	25.13(0.10)
P1–N1	1.595(2)	O1–Y1–O2	102.03(7)		

Table 5. Data for the ROP of Lactide Using Yttrium Initiators 1–3 $[LA]_0 = 1 M$

initiator (I)	$[LA]_0/[I]$ or $[LA]_0/[I]:[iPrOH]$	time	conversion ^a /%	$M_n(\text{calcd})^b/\text{kg mol}^{-1}$	$M_n(\text{exp})^c/\text{kg mol}^{-1}$	PDI ^e	P_s^d	k_{obs}^e
1	200:1	3360 s (56 min)	90	25.9	27.1	1.36	0.78	0.0031 ^f
2	200:1	40 s	91	26.2	57.6	1.42	0.78	0.2522 ^f
3	200:1	5 s	98	28.8	64.6 ^g	1.20 ^g	0.86 ^g	
3	1000:1	45 s	97	140	223	1.34	0.86	0.0799 ^g
3	1000:1:1	70 s	80	115	105	1.08	0.90	
3 ^h	1000:1	120 s ^k	99	144	332	1.31	0.87	
3 ⁱ	2000:1	10 min ^k	99	288	330	1.35	0.87	
3 ^j	5000:1	30 min ^k	98	720	700	1.23	0.88	

^aConversions were determined from the ¹H NMR spectra (CDCl₃) of the crude products by integration of the methine resonance assigned to LA ($\delta = 4.92$ ppm) and PLA ($\delta = 5.00$ – 5.30 ppm). ^b $M_n(\text{calcd}) = 144[LA]_0/[I] \times \% \text{ conversion LA}$. ^c $M_n(\text{exp})$ was determined using GPC, in THF, using multiangle laser light scattering (GPC-MALLS) according to the method described earlier.^{12ij} The polydispersity index was also determined from GPC, $PDI = M_w/M_n$. ^d P_s is the probability of racemic linkages between monomer units and is determined by comparison of the integrals of tetrads in the homonuclear decoupled ¹H NMR spectrum with those calculated using Bernoullian statistics according to the method described by Coudane et al.¹⁵ ^eDetermined from the gradients of the $\ln\{[LA]_0/[LA]_t\}$ (for first-order reaction) or $1/[LA]_t$ (for second-order reaction) versus time plots. ^fExpressed in $M^{-1}s^{-1}$. The reaction is second order in lactide. ^gExpressed in s^{-1} . The reaction is first order in lactide, $[I] = 1 \text{ mM}$. ^hReaction using unpurified lactide. ⁱSlurry of 2 mmol of lactide in 1 mL THF at 25 °C. ^jSlurry of 5 mmol of lactide in 1 mL THF at 25 °C. ^kReaction time unoptimized. ^lThis experiment showed a rapid increase of PDI and decrease of P_s over time.

Figure 5. Relevant reported yttrium salen and semisalen initiators.^{2d,12q,r,13c}Figure 6. $\ln\{[LA]_0/[LA]_t\}$ versus time for LA ROP using initiator 3. Polymerization conditions: $[LA]_0 = 1 M$, $[3] = 1 \text{ mM}$, THF, 25 °C.

to test this and to bring the experimental M_n close to its calculated values, an experiment was carried out where an equivalent of isopropyl alcohol was added. A yttrium isopropoxide complex is expected to be a better initiator due to its reduced steric hindrance and is also a good model for the secondary alkoxide propagating species. Addition of an equivalent of isopropyl alcohol led to improved control, as evidenced by the excellent agreement between the experimentally determined and the calculated values for M_n and the

PDI being below 1.10 in almost all samples (Figure 7). These results indicate that isopropyl alcohol is a viable chain transfer agent and a more effective initiator. Examination of the MALDI-ToF MS of the PLA produced from the initiating system comprising 3 and *i*PrOH shows two series of chains, one end-capped with *tert*-butoxyester and hydroxyl groups and the other end capped with isopropylester and hydroxyl groups (Figure S7 of the Supporting Information).

VT-NMR experiments were carried out to investigate formation of a yttrium isopropoxide complex upon addition of isopropanol (1 equiv) and its exchange with the alcohol in solution; detailed results are presented in the Supporting Information (Figures S12–15). Formation of an LY*O**i*Pr complex and its rapid exchange with free *t*BuOH was demonstrated. As isopropoxide is a better initiating group than *tert*-butoxide, the equilibrium between LY*O**i*Pr and LY*O**t*Bu is driven toward formation of the isopropoxide complex during reaction. Moreover, HO*t*Bu is a poor chain transfer agent. Taking into account all data, polymerizations are expected to be dominated by the yttrium isopropoxide initiator.

Initiators 1 and 2. Complexes 1 and 2 also showed good activity for the ROP of lactide, although they were somewhat slower than complex 3. Comparing the time taken to reach complete conversion at 5 mM initiator loading complex 1 required 3500 s, 2 took 40 s, and 3 needed just 5 s. Polymerizations using 1 and 2 were analyzed by taking aliquots throughout polymerizations.

Analysis of the kinetics for polymerization was undertaken using initiator 2 (Figure 8). This species showed complex kinetic behavior, with a second-order dependence on lactide concentration and a third-order dependence on yttrium concentration. Such data are indicative of substantial

Table 6. Data for the ROP of Lactide Using Yttrium Initiators 3–6

initiator (I)	$[LA]_0/[I]$	time	conversion ^a / %	$M_n(\text{calcd})^b/\text{kg mol}^{-1}$	$M_n(\text{exp})^c/\text{kg mol}^{-1}$	PDI ^c	P_s^d
3	1000:1	45 s	97	140	223	1.34	0.86
3 ^e	2000:1	10 min ^g	99	288	330	1.35	0.87
3 ^f	5000:1	30 min ^g	98	720	700	1.23	0.88
4 ^{12r}	500:1	40 min	90	72	93	1.13	
5 ^{13c}	300:1	60 min	>98	43	37	1.64	0.65
6 ^{2d}	100:1	14 h	>98				
7 ^{12q}	100:1	3 days	80	12	10	1.18	0.72

^aConversions were determined from the ¹H NMR spectra (CDCl₃) of the crude products by integration of the methine resonance assigned to LA ($\delta = 4.92$ ppm) and PLA ($\delta = 5.00$ – 5.30 ppm). ^b $M_n(\text{calcd}) = 144[LA]_0/[I] \times \%$ conversion LA. ^c $M_n(\text{exp})$ was determined using GPC, in THF, using multiangle laser light scattering (GPC-MALLS) according to the method described earlier.^{12i,j} The polydispersity index was also determined from GPC, $PDI = M_w/M_n$. ^d P_s is the probability of racemic linkages between monomer units and determined by comparison of the integrals of tetrads in the homonuclear decoupled ¹H NMR spectrum with those calculated using Bernoullian statistics, according to the method described by Coudane et al.¹⁵ ^eSlurry of 2 mmol of lactide in 1 mL of THF at 25 °C. ^fSlurry of 5 mmol of lactide in 1 mL of THF at 25 °C. ^gReaction time unoptimized

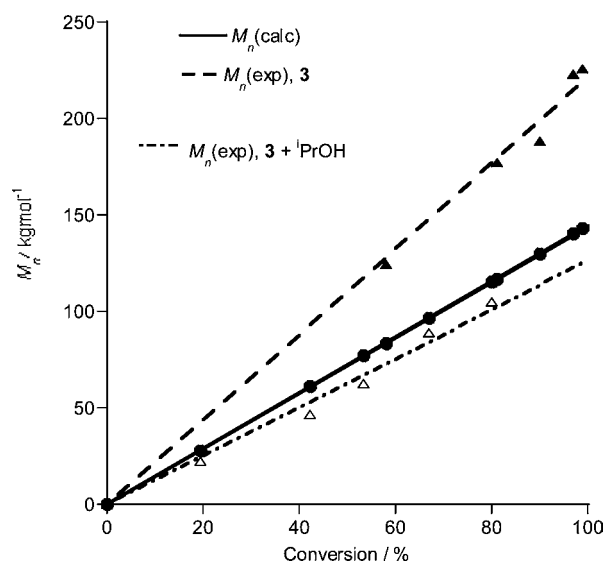


Figure 7. Evolution of M_n (kg/mol) versus conversion (%) for LA ROP using 3 (filled triangles) and with an extra equivalent of *i*PrOH (hollow triangles). Also plotted is $M_n(\text{calcd})$ (filled circles). Polymerization conditions: $[LA]_0 = 1$ M, $[3] = [i\text{PrOH}] = 1$ mM, THF, 25 °C.

aggregation occurring under the conditions of the catalysis and underscore the importance of the phosphasalen ancillary ligand structure. The kinetics were not monitored in detail for complex 1, due to its relatively slower rate, but preliminary investigations showed a related second-order dependence on lactide concentration (Figure S1, Supporting Information).

Polymerizations using complex 1 were well controlled, as shown by the linear evolution in the molecular weight with conversion and the narrow PDI for the PLA (Figure S2, Supporting Information). There was a good agreement between $M_n(\text{calcd})$ and $M_n(\text{exp})$, suggesting both alkoxide groups initiate polymerization. On the other hand, for complex 2 the $M_n(\text{exp})$ values were approximately double the $M_n(\text{calcd})$ values on the basis of a dinuclear structure (Figure S3, Supporting Information). In situ ³¹P{¹H} NMR spectroscopy was used to monitor a mixture of complex 2 and 25 equiv of LA. The spectrum was quite different from complex 2 alone; it showed four nonequivalent phosphorus nuclei (Figure S11, Supporting Information), data which could support aggregation under the conditions of the catalysis. Currently, we are unable to unambiguously assign the solution structure of complex 2 under the polymerization conditions. However, the complex

behaviors of 1 and 2 are in direct contrast with complex 3, with bulky substituents on the phosphasalen ligand, which accelerates the rate and prevents catalyst aggregation.

PLA Tacticity. The polylactide produced from *rac*-lactide using the three initiators shows a heterotactic bias (P_s). Determination of P_s was carried out using the probabilities calculated by Coudane et al.;¹⁵ every tetrad signal was analyzed and the average value for P_s reported (for all spectra see Figures 9 and S8–10 in the Supporting Information). PLA produced using initiators 1 and 2 had P_s values in the range 0.78–0.81, regardless of the *rac*-LA conversion or initiator concentration.

Complex 3 shows considerably enhanced heteroselectivity with P_s 0.86–0.90. Once again, the probability of heterotactic enchainment was independent of the conversion of *rac*-LA, addition of isopropyl alcohol, or concentration of the initiator. It is quite interesting to observe that highly heterotactic PLA was produced from either purified or crude LA. As an illustration of the high degrees of heteroselectivity conferred by this initiator, the methyne region of the ¹H NMR spectrum of PLA (Figure 9, at 98% conversion of LA) is illustrated; it is dominated by two quartets, assigned to heterotactic PLA (Figure 9 also shows the homonuclear decoupled NMR spectrum with the tetrad assignment and P_s value).

Discussion. Complexes 1 and 2 initiate and propagate ROP via a coordination insertion mechanism. The MALDI-ToF MS of the PLA produced using these initiators shows chains end capped with ethyl ester and *tert*-butyl ester groups, respectively (as well as the expected hydroxyl group at the opposite chain end, consistent with this mechanism, see Figures S4 and S5, Supporting Information). Both complexes exhibit dinuclear structures in the solid state, with complex 1 having bridging ethoxide groups while complex 2 bridges through a phenolate group from each phosphasalen ligand. Both complexes are viable initiators, but 1 is significantly slower than 2. Indeed, at 5 mM initiator concentration, complete conversion was observed after approximately 1 h using complex 1 and after only 40 s using complex 2. Both initiators display complex polymerization kinetics, consistent with second-order dependencies on lactide concentration and aggregation of the yttrium complexes. This motivated study of more sterically hindered phosphasalen ligands.

Complex 3 was prepared from a phosphasalen ligand having sterically hindered *tert*-butyl substituents on the phenol ring. On the basis of NMR data and the solid-state structure, it is proposed that this species retains a mononuclear structure in solution. Polymerizations using this initiator showed extremely

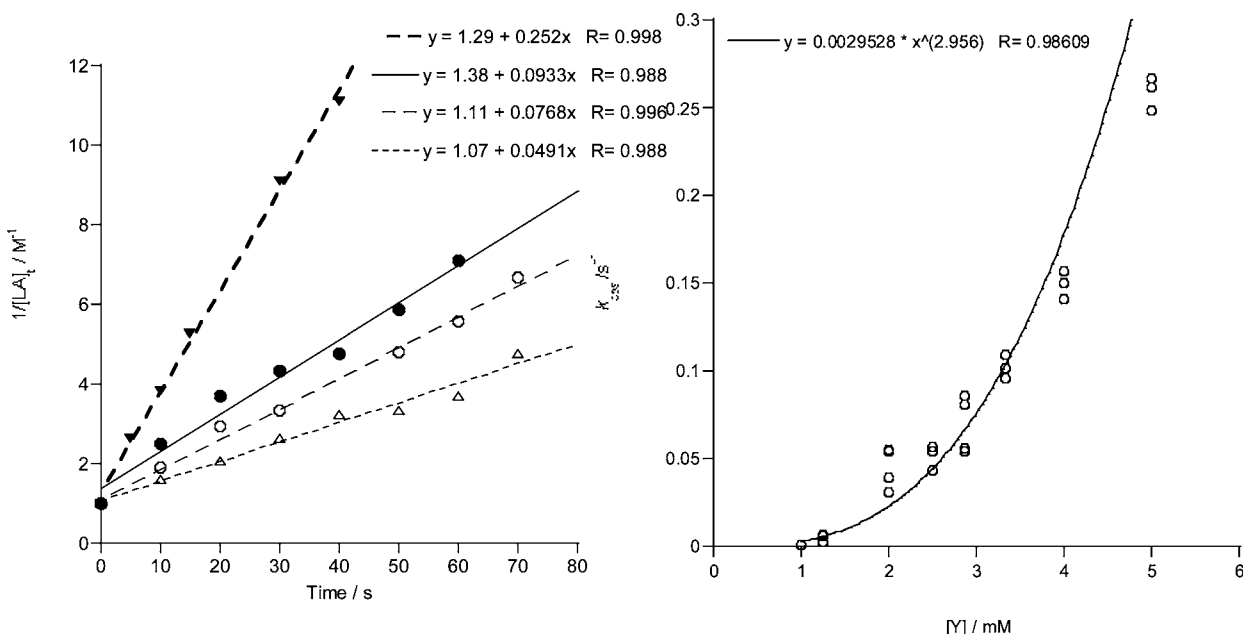


Figure 8. Plot showing $1/[LA]_t$ (M^{-1}) versus time (s) for LA ROP using **2** over the concentration range 2.5–5 mM. Polymerization conditions: $[LA]_0 = 1$ M, THF, 25 °C, $[2] = 5$ mM (filled triangles, $k_{obs} = 0.252$ $M^{-1} s^{-1}$); $[2] = 3.3$ mM (filled circles, $k_{obs} = 0.0933$ $M^{-1} s^{-1}$); $[2] = 2.9$ mM (open circles, $k_{obs} = 0.0768$ $M^{-1} s^{-1}$); $[2] = 2.5$ mM (open triangles, $k_{obs} = 0.0491$ $M^{-1} s^{-1}$). RHS: Plot of k_{obs} versus $[Y]$, polymerization conditions; $[LA]_0 = 1$ M, THF, 25 °C, $[2] = 1$ –5 mM.

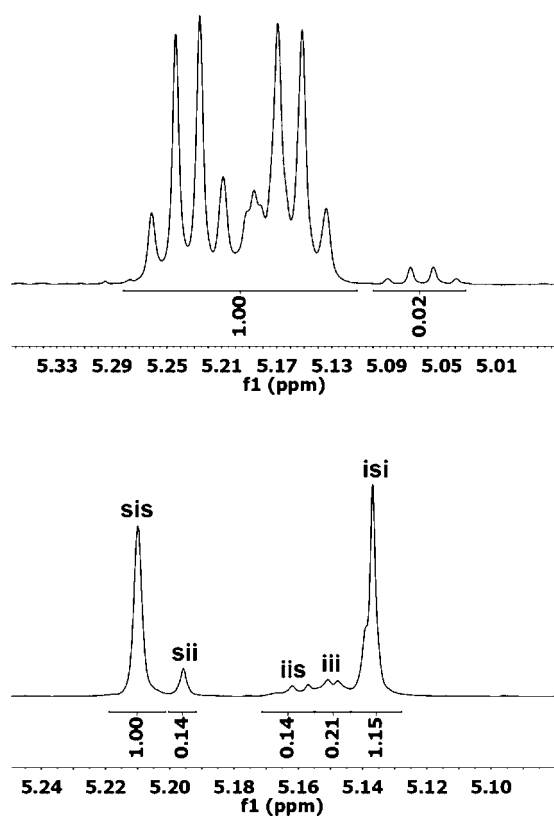


Figure 9. 1H and $^1H\{^1H\}$ NMR spectrum of PLA in $CDCl_3$; $[LA]_0 = 1$ M, $[3] = 1$ mM, $[iPrOH] = 1.2$ mM, 98% conversion of LA, THF, 25 °C, $P_s = 0.88$.²⁰

rapid rates; indeed, the pseudo-first-order rate constant (at $[3] = 1$ mM) is very high ($k_{obs} = 0.08$ s^{-1}), and the rate depends to the first order on the concentration of LA. A mixture of complex **3** and 25 equiv of LA was analyzed by $^{31}P\{^1H\}$ NMR

spectroscopy; it showed that the ligand remained coordinated to the yttrium centers, ruling out ligand dissociation during catalysis. Furthermore, complex **3** showed excellent heteroselectivity for *rac*-LA ROP. This interesting finding further confirms earlier experiments using bis(phosphinic amido) yttrium complexes, where high degrees of heteroselectivity were only observed from a mononuclear complex.^{12j} Stereocontrol is proposed to arise via a chain end control mechanism, that is, where the stereochemistry of the last inserted lactide unit controls the stereochemistry of the coordination/insertion into the next lactide unit. Our group and others previously observed enhanced stereocontrol for yttrium initiators in THF.^{12g,j,t,21} An NMR-scale experiment involving addition of increasing quantities of THF to a solution of **3** in toluene did not lead to a significant shift in the THF resonances due to either rapid exchange or a lack of coordination. It is, however, clear that the THF solvent is important for the high stereocontrol as an experiment conducted in toluene ($[LA] = 1$ M, $[3] = 1$ mM, in toluene, 80 °C, 91% conversion) yielded a PLA with much lower heteroselectivity ($P_s = 0.73$ vs 0.89 in pure THF).

Coates^{2d} and Carpentier^{12q} both studied yttrium complexes of (substituted) tetradentate salen ligands (Figure 5, 6 and 7). The yttrium complexes, either as mono- or dinuclear complexes (bridging through the alkoxide group), were not particularly active in lactide ROP, and limited stereocontrol was reported. These phosphasalén yttrium complexes show markedly different behavior, giving very high activities for lactide polymerization and high heteroselectivity for *rac*-LA ROP. The electronic properties of the iminophosphorane functional group in the phosphasalén ligand differ notably from the imine moiety in the salen analogue. NBO (natural bond orbital) analyses were performed on the structures of model compounds optimized using density functional theory with B3PW91 as the functional and the 6-31G* basis set; these calculations underline the divergent electronic properties of the

ligands (Figure 10). Whereas the charge difference between the C and the N of an imine remain low ($|\Delta q| = 0.51$), there is a

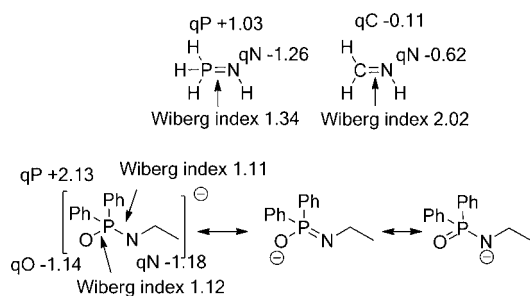


Figure 10. Comparisons of the Wiberg indices and NBO charge for various model compounds calculated using Gaussian09 using the B3PW91 functional and 6-31G* basis set.

pronounced difference between the phosphorus and the nitrogen atoms of an iminophosphorane ($|\Delta q| = 2.29$). This indicates that the iminophosphorane adopts a dipolar structure, which is further confirmed by the Wiberg bond indices, which were calculated at 1.34 for the P–N bond vs 2.02 for the C–N of the imine. Therefore, there is no double bond and no π system in an iminophosphorane. Thus, they should be seen as $P^+–N^-$ instead of the conventional $P=N$, the P–N bonding being enforced by negative hyperconjugation.²² Upon coordination, the iminophosphorane ligands behave as strong π and σ donors.

With this in mind, it is interesting to re-examine a series of initiators our group previously studied: the bis(phosphinic)-diamido yttrium complexes. The compounds show excellent activities in lactide polymerization.^{12i,j,l} All complexes were highly active; furthermore, a monomeric complex gave heterotactic PLA ($P_s = 0.85$). All complexes have tetradentate bis(phosphinic amido) ancillary ligands coordinated to the yttrium centers via the N and O atoms. NBO analysis performed on a model of diphenylphosphinic amido derivative shows some similarities with iminophosphorane derivatives (Figure 10). Indeed, the NBO charges at P, N, and O were calculated at +2.13, –1.18, and –1.14, respectively. Moreover, both the P–N and the P–O bond indices are close to 1. This is in agreement with the existence of two resonance forms for this functionality, one of which corresponds to an iminophosphorane ($N=P–O^-$). The X-ray crystal structures of these complexes show that the P–N bond lengths and geometries at the P and N centers fit with the ligands having some degree of iminophosphorane functionality (Figure 11, Table 7).

Experimentally, it appears that this iminophosphorane ligand motif accelerates ROP at the yttrium centers, leading to much enhanced activities and even enabling stereochemical control.

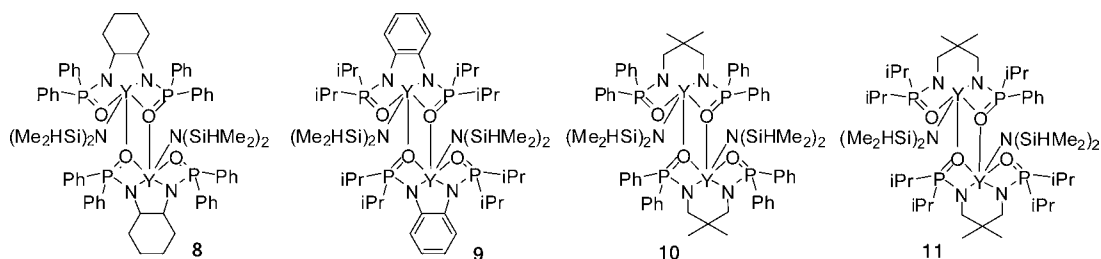


Figure 11. Dimeric bis(phosphinic amido)^{12i,l} yttrium complexes.

The iminophosphorane functionality is significantly more electron donating than the imine analogue in the salen ligand. In lactide ROP, there is a balance between requiring a Lewis-acidic yttrium center to facilitate lactide coordination while also requiring a labile yttrium alkoxide bond to accelerate insertion of the lactide unit. Thus, it seems that a better donor ligand is desirable; this may be due to weakening or labilizing of the yttrium–alkoxide bond and acceleration of the insertion step. Diaconescu and co-workers recently reported a switchable activity in lactide ROP using an yttrium alkoxide complex with a tetradentate ligand featuring in the backbone an iminophosphorane linked to a ferrocene.^{5b} Whereas the complex bearing the neutral (reduced) ligand with an electron-rich nitrogen donor group is active for the ROP of lactide, the oxidized complex (featuring a ferrocenium) is completely inactive. Thus, polymerization activity is switched ‘off’ when the electron density at the nitrogen decreases. It was hypothesized that although insertion of the monomer to the oxidized complex is possible, propagation from such a species is unfavorable, since the alkoxide would be connected to a more electron-deficient metal. This observation strongly supports the benefit of a good donor ligand for the ROP of lactide. The flexibility of the ligand could also play an important role as the coordination geometry at yttrium is expected to change during the coordination–insertion steps in ROP, and a more flexible ligand could be beneficial; some theoretical studies supporting this notion have been reported.²³

CONCLUSIONS

Three yttrium alkoxide complexes featuring a new class of phosphasalen ligands have been synthesized and characterized by multinuclear NMR techniques, elemental analysis, and X-ray diffraction experiments. All three complexes are highly active initiators for *rac*-lactide ring-opening polymerization and display good polymerization control and good/excellent heteroselectivity. The order of activity of the complexes spans $3 > 2 \gg 1$ with all complexes displaying excellent rates but complex 3 being particularly fast and able to polymerize unpurified lactide to complete conversion within seconds. It is notable that all phosphasalen yttrium complexes display significantly greater activity than the analogous yttrium salen complexes. All polymerizations are well controlled; the number-averaged molecular weight increases linearly with conversion, show good fits with the calculated molecular weights, and the polydispersity indices are moderate/narrow. Furthermore, all complexes produce heterotactic PLA, with P_s values up to 0.9 in the case of 3. The high polymerization activities can be rationalized by the electronic properties of the ligands: iminophosphorane ligands are considerably more electron donating than their salen analogues. In lactide polymerization there are two important processes that the metal active site

Table 7. Structural Data for Dimeric Bis(phosphinic amido)^{12i,1} and Phosphasalen Yttrium Complexes (Y–N and Y–O distances relative to ancillary ligand)

complex	P–N (Å)	Y–N (Å)	Y–O (Å)
8 ¹²ⁱ	1.576(2), 1.568(2)	2.336(2), 2.395(2)	2.3336(17), 2.4444(16)
9 ¹²ⁱ	1.5907(18), 1.5989(18)	2.3560(17), 2.3348(17)	2.3409(15), 2.4720(13)
10 ¹²ⁱ	1.5922(13), 1.5821(12)	2.3681(12), 2.3542(12),	2.3548(10), 2.4621(10)
11 ¹²ⁱ	1.596(6), 1.582(6)	2.216(6), 2.345(6)	2.315(5), 2.524(5)
1	1.598(3), 1.595(3)	2.415(3), 2.438(3)	2.182(3), 2.213(3),
2	1.596(3), 1.586(3)	2.398(3), 2.372(3)	2.203(3), 2.338(2),
3	1.595(2), 1.584(2)	2.375(2), 2.324(2)	2.1671(318), 2.1704(18)

controls: coordination of the lactide, which is governed by the Lewis acidity of the metal center, and insertion of the lactide into the metal alkoxide bond, which is governed by the lability/nucleophilicity of that alkoxide. It is therefore of significant interest to note that more electron-donating ligands, such as these phosphasalen ligands or the bis(phosphinic amido) ligands previously described by our group, are very well suited to preparation of highly active polymerization initiators. This could be due to an increase in the lability of the yttrium alkoxide bond; further investigations will aim to uncover the structure–activity relationships of this interesting new class of ligand. Furthermore, metal–salen complexes have found a very wide range of catalytic applications, far beyond lactide polymerization; this report highlights the potential impact of phosphasalen analogues on a range of other catalyzes.

EXPERIMENTAL SECTION

Materials and Methods. All reactions were conducted under an atmosphere of dry nitrogen or argon using standard Schlenk and glovebox techniques. Solvents and reagents were obtained from commercial sources. Tetrahydrofuran, toluene, pentane, hexane, and petroleum ether were distilled from sodium/benzophenone under dry nitrogen. Dichloromethane was distilled from CaH₂ under dry nitrogen. *rac*-Lactide was recrystallized from anhydrous toluene and sublimed three times prior to use. [YCl₃(THF)_{3,5}]²⁴ and phosphinophenols²⁵ were prepared following literature procedure.

Measurements. Nuclear magnetic resonance (NMR) spectra were recorded on a Bruker Av300 spectrometer operating at 300 MHz for ¹H, 75.5 MHz for ¹³C{¹H}, and 121.5 MHz for ³¹P{¹H}. Solvent peaks were used as internal references for ¹H and ¹³C chemical shifts (ppm). ³¹P peaks were referenced to external 85% H₃PO₄. When needed, higher resolution ³¹P{¹H} NMR and ¹H{¹H} NMR (homodecoupled spectroscopy) experiments were performed on a Bruker Av500 spectrometer, equipped with a z-gradient bbo/5 mm tunable probe and a BSMS GAB 10 A gradient amplifier providing a maximum gradient output of 5.35 G/cmA. ¹H NMR spectra for all lactide polymerizations were performed on a Bruker Av400 instrument. The following abbreviations are used: br, broad; s, singlet; d, doublet; dd, doublet of doublets; t, triplet; m, multiplet; v, virtual. The labeling schemes of the phosphasalen ligands and complexes are given in Schemes 1 and 2.

Elemental analyses were determined by Mr. Stephen Boyer at London Metropolitan University, Science Centre, 29 Hornsey Road, London N7 7DD. Mass spectra were performed on a Micromass MALDI-ToF micro MX using potassium salts for ionization. The PLA number-averaged molecular weight, *M_n*, and polydispersity index (*M_w*/*M_n*; PDI) were determined using gel permeation chromatography equipped with multiangle laser light scattering (GPC-MALLS). Two Polymer Laboratories Mixed D columns were used in series with THF as the eluent at a flow rate of 1 mL min⁻¹ on a Polymer Laboratories PL GPC-50 instrument at 35 °C. The light scattering detector was a triple-angle detector (Dawn 8, Wyatt Technology), and data were analyzed using Astra V version 5.3.4.18. The refractive angle increment for polylactide (dn/dc) in THF was 0.042 mL g⁻¹.²⁶

Synthesis of S1 and S2. At –78 °C, bromine (200 μL, 3.88 mmol) was added dropwise to a solution of the appropriate phenolphosphine (1.52 g, 3.88 mmol) in CH₂Cl₂ (30 mL). The cold bath was removed, and stirring was continued for 45 min at 25 °C; subsequently, the solution was cooled to –78 °C. Bu₃N (926 μL, 3.88 mmol) was added, followed by ethylene diamine (130 μL, 1.94 mmol), and the solution was allowed to warm to 25 °C. After 16 h, a cloudy yellow solution was formed, from which the solvents were evaporated and THF (15 mL) was added. A white slurry was formed with sonification, and the white product was isolated by filtration, washed with THF (5 × 7 mL), and dried in vacuum.

S1: 0.98 g, 1.26 mmol, 65%. ³¹P{¹H} NMR (CDCl₃): δ 39.3 (s, P^V). ¹H NMR (CDCl₃): δ 7.67–7.59 (12H, m, *p*-CH(PPh₂), *o*-CH(PPh₂)), 7.52–7.46 (12H, m, *m*-CH(PPh₂), C_aH, C_bH), 6.86–6.75 (4H, m, C_cH, NH), 6.57 (2H, dd, ³J_{H,H} = 8.0 Hz, ³J_{P,H} = 14.5 Hz, C_dH), 3.43 (4H, d, ³J_{P,H} = 10.5 Hz, CH₂). ¹³C{¹H} NMR (CDCl₃): δ 159.7 (d, ²J_{P,C} = 0.5 Hz, OC^{IV}), 136.1 (d, ⁴J_{P,C} = 1.0 Hz, C_bH), 133.3 (d, ²J_{P,C} = 11.5 Hz, C_dH), 133.1 (d, ⁴J_{P,C} = 3.0 Hz, *p*-CH(PPh₂)), 131.9 (d, ²J_{P,C} = 11.5 Hz, *o*-CH(PPh₂)), 128.5 (d, ³J_{P,C} = 13.5 Hz, *m*-CH(PPh₂)), 121.4 (d, ¹J_{P,C} = 106.5 Hz, C^{IV}(PPh₂)), 119.6 (d, ³J_{P,C} = 13.5 Hz, C_cH), 117.7 (d, ³J_{P,C} = 7.0 Hz, C_aH), 106.8 (d, ²J_{P,C} = 104.0 Hz, PPh₂C^{IV}), 43.3 (d, ²J_{P,C} = 1.5 Hz, CH₂). HR-EI-MS: 307.1132 ([M – 2Br]²⁺; C₃₈H₃₆N₂O₂P₂); calcd 307.1126.

S2·THF: 1.47 g, 1.37 mmol, 71%. ³¹P{¹H} NMR (CDCl₃): δ 40.3 (s, P^V). ¹H NMR (CDCl₃): δ 8.15 (b, 2H, CH(PPh₂)), 7.75–7.56 (m, 18H, CH(PPh₂)), 6.93 (b, 2H, C_bH), 6.44 (dd, ⁴J_{H,H} = 2.1 Hz, ³J_{P,H} = 15.2 Hz, 2H, C=H), 3.78 (m, 4H, O–CH₂(THF)), 3.74 (b, 4H, N–CH₂–CH₂–N), 1.85 (m, 4H, O–CH₂–CH₂(THF)), 1.59 (b, 2H, OH), 1.52 (s, 18H, C_a–C(CH₃)₃), 1.08 (s, 18H, C_c–C(CH₃)₃).

The insolubility of the product in all regular deuterated solvents prevents ¹³C{¹H} NMR characterization.

Synthesis of L1 and L2. KHMDS (7.0 g, 35.1 mmol) was added to a suspension of the aminophosphonium salt (8.8 mmol) in THF (320 mL) at ambient temperature. After 16 h, a cloudy solution was formed. The white potassium bromide byproduct was removed by centrifugation. Solvent was removed in vacuo, and the residue was dissolved in petroleum ether (60 mL). After 5 min of sonification, a white slurry was formed. The white solid was separated by centrifugation, washed with petroleum ether (20 mL), and dried in vacuo.

L1: 6.0 g, 8.7 mmol, 99%. ³¹P{¹H} NMR (THF-*d*₈): δ 18.6 (s, P^V). ¹H NMR (THF-*d*₈): δ 7.73–7.67 (m, 8H, *o*-CH(PPh₂)), 7.62–7.57 (m, ⁵J_{P,H} = 1.5 Hz, 4H, *p*-CH(PPh₂)), 7.55–7.49 (d, ⁴J_{P,H} = 2.0 Hz, 8H, *m*-CH(PPh₂)), 7.09 (m, 2H, ³J_{H,H} = 8.5 Hz, ³J_{P,H} = 7.0 Hz, ⁴J_{H,H} = 1.5 Hz, 2H, C_bH), 6.6.61 (m, 2H, ³J_{H,H} = 8.5 Hz, 2H, C_aH), 6.47 (ddd, ⁴J_{H,H} = 1.5 Hz, ³J_{H,H} = 7.0 Hz, ³J_{P,H} = 16.0 Hz, 2H, C_cH), 6.05 (ddd, ³J_{H,H} = ³J_{P,H} = 7.0 Hz, ⁴J_{P,H} = 3.0 Hz, 2H, C_cH), 3.42 (dd, ³J_{P,H} = 6.0 Hz, ³J_{P,H} = 6.5 Hz, 4H, N–CH₂–CH₂–N). ¹³C{¹H} NMR (THF-*d*₈): δ 174.3 (d, ²J_{P,C} = 3.5 Hz, O–C^{IV}), 132.9 (d, ²J_{P,C} = 13.0 Hz, C_dH), 132.8 (d, ¹J_{P,C} = 77.0 Hz, C^{IV}(PPh₂)), 132.1 (d, ⁴J_{P,C} = 1.3 Hz, C_bH), 131.7 (²J_{P,C} = 8.0 Hz, *o*-CH(PPh₂)), 129.0 (d, ⁴J_{P,C} = 2.0 Hz, *p*-CH(PPh₂)), 127.0 (d, ³J_{P,C} = 10.5 Hz, *m*-CH(PPh₂)), 121.8 (d, ³J_{P,C} = 9.0 Hz, C_aH), 112.5 (d, ¹J_{P,C} = 128.7 Hz, C^{IV}–PPh₂), 107.0 (d, ³J_{P,C} = 15.2 Hz, C_cH), 50.4 (dd, ²J_{P,C} = 27.0 Hz, ³J_{P,C} = 8.0 Hz, N–CH₂–CH₂–N). Anal. Calcd for C₃₈H₃₂K₂N₂O₂P₂: C, 66.26; H, 4.68; N, 4.07. Found: C, 66.19; H, 4.73; N, 3.99.

L2t·2THF: 7.2 g, 6.8 mmol, 78%. $^{31}\text{P}\{^1\text{H}\}$ NMR (THF- d_8): δ 20.6 (s, P^V). ^1H NMR (toluene- d_6): δ 7.52–7.50 (m, 10H, CH(PPh₂) + C₆H), 7.05–7.01 (m, 12H, CH(PPh₂)), 6.30 (dd, $^3J_{\text{H,H}} = 2.5$ Hz, $^3J_{\text{P,H}} = 17.0$ Hz, 2H, C₆H), 3.41–3.38 (m, 8H, O–CH₂(THF)), 3.20 (vt, $J_{\text{P,H}} = J_{\text{P,H}} = 5.0$ Hz, 4H, N–CH₂–CH₂–N), 1.70 (s, 18H, C_a–C(CH₃)₃), 1.36 (m, 8H, O–CH₂–CH₂(THF)), 1.08 (s, 18H, C_c–C(CH₃)₃). $^{13}\text{C}\{^1\text{H}\}$ NMR (THF- d_8): δ 173.4 (d, $^2J_{\text{P,C}} = 4.0$ Hz, C^{IV}–O), 140.1 (d, $^3J_{\text{P,C}} = 9.5$ Hz, C_c^{IV}), 134.2 (d, $^1J_{\text{P,C}} = 81.5$ Hz, C^{IV}(PPh₂)), 133.7 (d, $^{2/3}J_{\text{P,C}} = 7.5$ Hz, *o*- or *m*-CH(PPh₂)), 130.5 (d, $^4J_{\text{P,C}} = 2.0$ Hz, *p*-CH(PPh₂)), 128.8 (d, $^2J_{\text{P,C}} = 15.5$ Hz, C_aH), 128.6 (d, $^3J_{\text{P,C}} = 17.0$ Hz, C_a^{IV}), 128.4 (d, $^{2/3}J_{\text{P,C}} = 10.5$ Hz, *o*- or *m*-CH(PPh₂)), 127.4 (d, $^4J_{\text{P,C}} = 1.0$ Hz, C_bH), 112.8 (d, $^1J_{\text{P,C}} = 134.0$ Hz, C^{IV}–PPh₂), 52.1 (dd, $J_{\text{P,C}} = 9.5$ Hz, $J_{\text{P,C}} = 29.5$ Hz, N–CH₂–CH₂–N), 36.0 (d, $^4J_{\text{P,C}} = 2.0$ Hz, C_a^{IV}–C(CH₃)₃), 34.0 (d, $^4J_{\text{P,C}} = 0.5$ Hz, C_c^{IV}–C(CH₃)₃), 31.9 (s, C(CH₃)₃), 29.9 (s, C(CH₃)₃). Anal. Calcd for C₆₂H₈₀K₂N₂O₄P₂: C, 70.42; H, 7.63; N, 2.65. Found: C, 70.57; H, 7.80; N, 2.49.

Synthesis of Yttrium Complexes. Complex 1. [YCl₃(THF)_{3.5}] (313 mg, 0.7 mmol) was added to a solution of L1 (491 mg, 0.7 mmol) in THF (30 mL) at –40 °C. A white slurry was formed after 2 min; stirring was continued at room temperature for 1 h. Potassium ethoxide (59 mg, 0.7 mmol) was added, giving a cloudy solution after 7 h. The solid was removed by centrifugation, and the filtrate was evaporated to give an off-white solid. Crystallization from toluene yielded the product as colorless crystals (430 mg, 0.59 mmol, 84%)

1: $^{31}\text{P}\{^1\text{H}\}$ NMR (THF- d_8): δ 29.3 (s, P^V). ^1H NMR (THF- d_8): δ 7.77–7.24 (m, 20H, CH(PPh₂)), 7.09 (dddd, $^3J_{\text{H,H}} = 8.7$ Hz, $^3J_{\text{H,H}} = 7.0$ Hz, $^4J_{\text{H,H}} = 1.7$ Hz, $^5J_{\text{P,H}} = 1.2$ Hz, 2H, C₆H), 6.79 (ddd, $^3J_{\text{H,H}} = 7.7$ Hz, $^4J_{\text{H,H}} = 1.7$ Hz, $^3J_{\text{P,H}} = 13.9$ Hz, 2H, C₆H), 6.52 (ddd, $^3J_{\text{H,H}} = 8.7$ Hz, $^4J_{\text{H,H}} = 0.7$ Hz, $^4J_{\text{P,H}} = 8.3$ Hz, 2H, C₆H), 6.31 (dddd, $^3J_{\text{H,H}} = 7.7$ Hz, $^3J_{\text{H,H}} = 7.0$ Hz, $^4J_{\text{H,H}} = 0.7$ Hz, $^4J_{\text{P,H}} = 3.5$ Hz, 2H, C₆H), 3.42 (b, 2H, O–CH₂–CH₃), 3.08 (b, 2H, N–CH₂–CH₂–N), 2.84 (b, 2H, N–CH₂–CH₂–N), 1.01 (b, 1H, O–CH₂–CH₃); 0.62 (b, 2H, O–CH₂–CH₃). $^{13}\text{C}\{^1\text{H}\}$ NMR (THF- d_8): δ 172.1 (d, $^3J_{\text{P,C}} = 2.3$ Hz, C^{IV}–O), 172.0 (d, $^3J_{\text{P,C}} = 2.7$ Hz, C^{IV}–O), 134.0 (s, *p*-CH(PPh₂)), 134.0 (d, $^{2/3}J_{\text{P,C}} = 9.5$ Hz, *o*- or *m*-CH(PPh₂)), 133.1 (d, $^4J_{\text{P,C}} = 10.9$ Hz, C₆H), 132.0 (m, C₆H); 131.8 (m, C(Ar)), 129.1 (m, C(Ar)), 122.7 (d, $^3J_{\text{P,C}} = 7.5$ Hz, C_aH), 114.9 (d, $^1J_{\text{P,C}} = 113.8$ Hz, C^{IV}–PPh₂), 113.0 (d, $^3J_{\text{P,C}} = 14.9$ Hz, C_aH), 51.3 (dd, $J_{\text{P,C}} = 6.3$ Hz, $J_{\text{P,C}} = 13.1$ Hz, N–CH₂–CH₂–N), 68.0 (s, O–CH₂–CH₃), 25.1 (s, O–CH₂–CH₃). Anal. Calcd for C₈₀H₇₄N₄O₆P₄Y₂: C, 64.52; H, 5.01; N, 3.76. Found: C, 64.44; H, 5.07; N, 3.72.

Complex 2. [YCl₃(THF)_{3.5}] (313 mg, 0.7 mmol) was added to a solution of L1 (491 mg, 0.7 mmol) in THF (50 mL) at –40 °C. A white slurry was formed after 2 min; stirring was continued at room temperature for 1 h. Potassium *tert*-butoxide (78.6 mg, 0.7 mmol) was added into the mixture, giving a cloudy solution after 7 h. Solid was removed by centrifugation. The solution was concentrated (to 10 mL). The product precipitated from solution as a white solid (380 mg, 0.49 mmol, 70%). Crystals suitable for X-ray diffraction experiments were obtained from a solution of complex 2 in THF/toluene (1/3 volume).

2: $^{31}\text{P}\{^1\text{H}\}$ NMR (THF- d_8): δ 30.4 (s, P^V). ^1H NMR (THF- d_8): δ 7.73–7.30 (m, 20H, CH(PPh₂)), 7.08 (dddd, $^3J_{\text{H,H}} = 8.7$ Hz, $^3J_{\text{H,H}} = 7.0$ Hz, $^4J_{\text{H,H}} = 1.7$ Hz, $^5J_{\text{P,H}} = 1.0$ Hz, 2H, C₆H), 6.53 (ddd, $^3J_{\text{H,H}} = 8.0$ Hz, $^4J_{\text{H,H}} = 1.7$ Hz, $^3J_{\text{P,H}} = 14.6$ Hz, 2H, C₆H), 6.50 (ddd, $^3J_{\text{H,H}} = 8.7$ Hz, $^4J_{\text{H,H}} = 1.0$ Hz, $^4J_{\text{P,H}} = 5.5$ Hz, 2H, C₆H), 6.18 (dddd, $^3J_{\text{H,H}} = 8.0$ Hz, $^3J_{\text{H,H}} = 7.0$ Hz, $^4J_{\text{H,H}} = 1.0$ Hz, $^4J_{\text{P,H}} = 3.5$ Hz, 2H, C₆H), 3.42 (b, 2H, O–CH₂–CH₃), 3.22 (b, 2H, N–CH₂–CH₂–N), 2.99 (b, 2H, N–CH₂–CH₂–N), 0.88 (b, 9H, O–C^{IV}(CH₃)₃). $^{13}\text{C}\{^1\text{H}\}$ NMR (THF- d_8): δ 172.7 (d, $^3J_{\text{P,C}} = 2.3$ Hz, C^{IV}–O), 172.6 (d, $^3J_{\text{P,C}} = 2.5$ Hz, C^{IV}–O), 134.0 (d, $^{2/3}J_{\text{P,C}} = 9.2$ Hz, *o*- or *m*-CH(PPh₂)), 134.0 (d, $^{2/3}J_{\text{P,C}} = 8.6$ Hz, *o*- or *m*-CH(PPh₂)), 133.1 (d, $^4J_{\text{P,C}} = 12.6$ Hz, C₆H), 131.8 (d, $^4J_{\text{P,C}} = 2.3$ Hz, *p*-CH(PPh₂)), 131.6 (d, $^1J_{\text{P,C}} = 74.6$ Hz, C^{IV}(PPh₂)), 131.5 (d, $^4J_{\text{P,C}} = 2.8$ Hz, C₆H), 131.5 (d, $^1J_{\text{P,C}} = 75.0$ Hz, C^{IV}(PPh₂)), 128.9 (d, $^{2/3}J_{\text{P,C}} = 11.5$ Hz, *o*- or *m*-CH(PPh₂)), 128.7 (d, $^{2/3}J_{\text{P,C}} = 10.7$ Hz, *o*- or *m*-CH(PPh₂)), 122.0 (d, $^3J_{\text{P,C}} = 8.0$ Hz, C_aH), 114.2 (d, $^1J_{\text{P,C}} = 121.3$ Hz, C^{IV}–P(Ph₂)), 112.4 (d, $^3J_{\text{P,C}} = 15.0$ Hz, C_aH), 68.0 (s, O–C^{IV}(CH₃)₃), 51.9 (dd, $J_{\text{P,C}} = 5.2$ Hz, $J_{\text{P,C}} = 15.5$ Hz, N–CH₂–CH₂–N), 32.7 (br. s, O–C^{IV}(CH₃)₃). Anal. Calcd for

C₈₄H₈₂N₄O₆P₄Y₂: C, 65.29; H, 5.35; N, 3.63. Found: C, 65.27; H, 5.25; N, 3.76.

Complex 3. [YCl₃(THF)_{3.5}] (313 mg, 0.7 mmol) was added to a solution of L2 (745 mg, 0.7 mmol) in THF (25 mL) at –40 °C. After 2 h of stirring at room temperature, potassium *tert*-butoxide (78.6 mg, 0.7 mmol) was added into the mixture, giving a cloudy solution. Stirring was continued for 7 h, and the solid was removed by centrifugation. Solvents were removed from the filtrate, yielding a pale yellow oil, which transformed into a white solid after 1 week of storing at room temperature (680 mg, 0.68 mmol, 97%). Monocrystals suitable for X-ray diffraction were grown from a saturated solution of complex 3 in cyclohexane.

3: $^{31}\text{P}\{^1\text{H}\}$ NMR (THF- d_8): δ 30.8 (s, P^V). ^1H NMR (THF- d_8): δ 7.57 (d, $^3J_{\text{H,H}} = 7.0$ Hz, $^3J_{\text{P,H}} = 11.2$ Hz, 4H, *o*-CH(PPh₂)), 7.61 (vt, $^3J_{\text{H,H}} = 7.0$ Hz, $^5J_{\text{P,H}} = 1.0$ Hz, 2H, *p*-CH(PPh₂)), 7.43 (vt, $^3J_{\text{H,H}} = 3J_{\text{H,H}} = 7.0$ Hz, 4H, *m*-CH(PPh₂)), 7.42 (dd, $^3J_{\text{H,H}} = 7.0$ Hz, $^3J_{\text{P,H}} = 10.7$ Hz, 4H, *o*-CH(PPh₂)), 7.42 (vt, $^3J_{\text{H,H}} = 7.0$ Hz, 2H, *p*-CH(PPh₂)), 7.34 (vtd, $^3J_{\text{H,H}} = 3J_{\text{H,H}} = 7.0$ Hz, $^4J_{\text{P,H}} = 2.5$ Hz, 4H, *m*-CH(PPh₂)), 7.28 (d, $^3J_{\text{H,H}} = 2.5$ Hz, 2H, C₆H), 6.34 (dd, $^3J_{\text{H,H}} = 2.5$ Hz, $^3J_{\text{P,H}} = 15.9$ Hz, 2H, C₆H), 3.31 (m, 2H, N–CH₂–CH₂–N), 3.18 (m, 2H, N–CH₂–CH₂–N), 1.37 (s, 18H, C_a–C(CH₃)₃), 0.98 (s, 18H, C_c–C(CH₃)₃), 0.68 (br. s, 9H, O–C(CH₃)₃). $^{13}\text{C}\{^1\text{H}\}$ NMR (THF- d_8): δ 169.7 (d, $^3J_{\text{P,C}} = 2.7$ Hz, C^{IV}–O), 139.0 (d, $^3J_{\text{P,C}} = 8.2$ Hz, C_c^{IV}); 134.0 (d, $^3J_{\text{P,C}} = 15.4$ Hz, C_a^{IV}), 134.1 (d, $^{2/3}J_{\text{P,C}} = 8.7$ Hz, *o*-CH(PPh₂)), 133.5 (d, $^{2/3}J_{\text{P,C}} = 8.9$ Hz, *o*-CH(PPh₂)), 132.7 (d, $^1J_{\text{P,C}} = 86.6$ Hz, C^{IV}(PPh₂)), 131.7 (d, $^1J_{\text{P,C}} = 89.0$ Hz, C^{IV}(PPh₂)), 131.9 (d, $^4J_{\text{P,C}} = 1.7$ Hz, *p*-CH(PPh₂)), 131.5 (d, $^4J_{\text{P,C}} = 1.8$ Hz, *p*-CH(PPh₂)), 128.9 (d, $^{2/3}J_{\text{P,C}} = 9.6$ Hz, *m*-CH(PPh₂)), 128.8 (d, $^{2/3}J_{\text{P,C}} = 10.0$ Hz, *m*-CH(PPh₂)), 128.3 (s, C₆H), 127.8 (d, $^2J_{\text{P,C}} = 13.9$ Hz, C_aH), 112.5 (d, $^1J_{\text{P,C}} = 122.2$ Hz, C^{IV}–PPh₂), 47.3 (dd, $J_{\text{P,C}} = 7.5$ Hz, $J_{\text{P,C}} = 19.0$ Hz, N–CH₂–CH₂–N), 35.8 (s, C_a^{IV}–C(CH₃)₃ + O–C(CH₃)₃), 34.3 (s, C_c^{IV}–C(CH₃)₃), 31.7 (s, C_c^{IV}–C(CH₃)₃ + O–C(CH₃)₃), 30.4 (s, C_a^{IV}–C(CH₃)₃). Anal. Calcd for C₅₈H₇₃N₂O₃P₂Y: C, 69.87; H, 7.38; N, 2.81. Found: C, 69.55; H, 7.26; N, 2.76.

General Procedure for Lactide Polymerization. To a rapidly stirred solution of *rac*-lactide (288 mg, 2 mmol) in THF, in a vial in the glovebox, was added the appropriate quantity of a solution of the initiator in tetrahydrofuran (0.01 M for complex 3, 0.02 M for complex 2, 0.1 M for complex 1); the overall concentration of *rac*-lactide was therefore kept at 1 M. Aliquots of the reaction mixture were taken at regular intervals, precipitated in hexane, and quenched in air. Solvent was allowed to evaporate slowly in air, yielding a crude product, which was analyzed by ^1H NMR spectroscopy (to determine % conversion) and GPC (to determine the M_n and PDI). The probability of syndiotactic linkages between monomer units (P_s) is determined from the homonuclear decoupled ^1H NMR spectrum: δ 5.14 and 5.22 ppm in CDCl₃ for heterotactic PLA.¹⁵

Kinetic Analyses. Reactions were monitored by taking aliquots and quenching with a large excess of hexane (which precipitates both PLA and any unreacted LA). This precipitation is expected to inhibit further polymerization (in combination with the high dilution, any polymerization which occurred after this quenching would be expected to do so very slowly). The vial was then immediately removed from the glovebox and exposed to air. Such conditions are sufficient to hydrolyze yttrium–alkoxide bonds (by reference to exposure of NMR samples of initiators to air) and stop polymerizations completely. Solvents were evaporated in air (overnight). Vacuum was not used to remove the solvents, so as to prevent any unintentional loss of lactide (through sublimation).

X-ray Crystallography. Data were collected at 150 K on a Bruker Kappa APEX II diffractometer using a Mo K α ($\lambda = 0.71069$ Å) X-ray source and a graphite monochromator. The crystal structure was solved using SIR 97²⁷ and Shelx1-97.²⁸ ORTEP drawings were made using ORTEP III for Windows.²⁹

■ ASSOCIATED CONTENT

Supporting Information

Additional kinetics plots; MALDI-ToF MS and $^1\text{H}\{^1\text{H}\}$ spectra of synthesized PLA; NMR studies on addition of isopropanol

to complex 3; computational details for model compounds. This material is available free of charge via the Internet at <http://pubs.acs.org>.

AUTHOR INFORMATION

Corresponding Author

*E-mail: audrey.auffrant@polytechnique.edu (A.A.); c.k.williams@imperial.ac.uk (C.K.W.).

Notes

The authors declare no competing financial interest.

REFERENCES

- (1) (a) Katsuki, T. *Coord. Chem. Rev.* **1995**, *140*, 189–214. (b) Tokunaga, M.; Larrow, J. F.; Kakiuchi, F.; Jacobsen, E. N. *Science* **1997**, *277* (5328), 936–938. (c) Jacobsen, E. N. *Acc. Chem. Res.* **2000**, *33* (6), 421–431. (d) Canali, L.; Sherrington, D. C. *Chem. Soc. Rev.* **1999**, *28* (2), 85–93. (e) Cozzi, P. G. *Chem. Soc. Rev.* **2004**, *33* (7), 410–421. (f) Melendez, J.; North, M.; Villuendas, P. *Chem. Commun.* **2009**, *18*, 2577–2579. (g) Haak, R. M.; Wezenberg, S. J.; Kleij, A. W. *Chem. Commun.* **2010**, *46* (16), 2713–2723.
- (2) (a) Spassky, N.; Wisniewski, M.; Pluta, C.; Le Borgne, A. *Macromol. Chem. Phys.* **1996**, *197*, 2627–2637. (b) Ovitt, T. M.; Coates, G. W. *J. Am. Chem. Soc.* **1999**, *121*, 4072–4073. (c) Jhurry, D.; Bhaw-Luximon, A.; Spassky, N. *Macromol. Symp.* **2001**, *175*, 67–79. (d) Ovitt, T. M.; Coates, G. W. *J. Am. Chem. Soc.* **2002**, *124* (7), 1316–1326. (e) Zhong, Z. Y.; Dijkstra, P. J.; Feijen, J. *Angew. Chem., Int. Ed.* **2002**, *41* (23), 4510–4513. (f) Nomura, N.; Ishii, R.; Akakura, M.; Aoi, K. *J. Am. Chem. Soc.* **2002**, *124*, 5938–5939. (g) Zhong, Z. Y.; Dijkstra, P. J.; Feijen, J. *J. Am. Chem. Soc.* **2003**, *125*, 11291–11298. (h) Hornmiron, P.; Marshall, E. L.; Gibson, V. C.; White, A. J. P.; Williams, D. J. *J. Am. Chem. Soc.* **2004**, *126*, 2688–2689. (i) Majerska, K.; Duda, A. *J. Am. Chem. Soc.* **2004**, *126*, 1026–1027. (j) Zelikoff, A. L.; Kopilov, J.; Goldberg, I.; Coates, G. W.; Kol, M. *Chem. Commun.* **2009**, *44*, 6804–6806. (k) Chisholm, M. H.; Patmore, N. J.; Zhou, Z. *Chem. Commun.* **2005**, 127–129.
- (3) (a) Hirahata, W.; Thomas, R. M.; Lobkovsky, E. B.; Coates, G. W. *J. Am. Chem. Soc.* **2008**, *130* (52), 17658–17659. (b) Ajiro, H.; Peretti, K. L.; Lobkovsky, E. B.; Coates, G. W. *Dalton Trans.* **2009**, *41*, 8828–8830. (c) Widger, P. C. B.; Ahmed, S. M.; Hirahata, W.; Thomas, R. M.; Lobkovsky, E. B.; Coates, G. W. *Chem. Commun.* **2010**, *46* (17), 2935–2937. (d) Thomas, R. M.; Widger, P. C. B.; Ahmed, S. M.; Jeske, R. C.; Hirahata, W.; Lobkovsky, E. B.; Coates, G. W. *J. Am. Chem. Soc.* **2010**, *132* (46), 16520–16525.
- (4) (a) Darensbourg, D. J.; Yarbrough, J. C. *J. Am. Chem. Soc.* **2002**, *124* (22), 6335–6342. (b) Qin, Z. Q.; Thomas, C. M.; Lee, S.; Coates, G. W. *Angew. Chem., Int. Ed.* **2003**, *42* (44), 5484–5487. (c) Darensbourg, D. J. *Chem. Rev.* **2007**, *107* (6), 2388–2410. (d) Nakano, K.; Nakamura, M.; Nozaki, K. *Macromolecules* **2009**, *42* (18), 6972–6980. (e) Darensbourg, D. J.; Ulusoy, M.; Karroonnirum, O.; Poland, R. R.; Reibenspies, J. H.; Cetinkaya, R. *Macromolecules* **2009**, *42* (18), 6992–6998. (f) Nakano, K.; Hashimoto, S.; Nozaki, K. *Chem. Sci.* **2010**, *1*, 369–373. (g) Coates, G. W.; Moore, D. R. *Angew. Chem., Int. Ed.* **2004**, *43* (48), 6618–6639. (h) Darensbourg, D. J.; Rodgers, J. L.; Mackiewicz, R. M.; Phelps, A. L. *Catal. Today* **2004**, *98* (4), 485–492. (i) Darensbourg, D. J.; Mackiewicz, R. M.; Rodgers, J. L.; Fang, C. C.; Billodeaux, D. R.; Reibenspies, J. H. *Inorg. Chem.* **2004**, *43* (19), 6024–6034. (j) Darensbourg, D. J.; Mackiewicz, R. M.; Rodgers, J. L.; Phelps, A. L. *Inorg. Chem.* **2004**, *43* (6), 1831–1833. (k) Luinstra, G. A.; Haas, G. R.; Molnar, F.; Bernhart, V.; Eberhardt, R.; Rieger, B. *Chem.—Eur. J.* **2005**, *11* (21), 6298–6314. (l) Darensbourg, D. J.; Phelps, A. L. *Inorg. Chem.* **2005**, *44* (13), 4622–4629. (m) Darensbourg, D. J.; Mackiewicz, R. M.; Billodeaux, D. R. *Organometallics* **2005**, *24* (1), 144–148. (n) Darensbourg, D. J.; Mackiewicz, R. M. *J. Am. Chem. Soc.* **2005**, *127* (40), 14026–14038. (o) Darensbourg, D. J.; Billodeaux, D. R. *Inorg. Chem.* **2005**, *44* (5), 1433–1442. (p) Chen, P.; Chisholm, M. H.; Gallucci, J. C.; Zhang, X.; Zhou, Z. *Inorg. Chem.* **2005**, *44* (8), 2588–2595. (q) Cohen, C. T.; Chu, T.; Coates, G. W. *J. Am. Chem. Soc.* **2005**, *127* (31), 10869–10878. (r) Cohen, C. T.; Thomas, C. M.; Peretti, K. L.; Lobkovsky, E. B.; Coates, G. W. *Dalton Trans.* **2006**, *1*, 237–249. (s) Darensbourg, D. J.; Ganguly, P.; Choi, W. *Inorg. Chem.* **2006**, *45* (10), 3831–3833. (t) Li, B.; Zhang, R.; Lu, X.-B. *Macromolecules* **2007**, *40* (7), 2303–2307. (u) Darensbourg, D. J.; Moncada, A. I. *Inorg. Chem.* **2008**, *47* (21), 10000–10008. (v) Na, S. J.; S., S.; Cyriac, A.; Kim, B. E.; Yoo, J.; Kang, Y. K.; Han, S. J.; Lee, C.; Lee, B. Y. *Inorg. Chem.* **2009**, *48* (21), 10455–10465.
- (5) (a) Broderick, E. M.; Thuy-Boun, P. S.; Guo, N.; Vogel, C. S.; Sutter, J.; Miller, J. T.; Meyer, K.; Diaconescu, P. L. *Inorg. Chem.* **2011**, *50* (7), 2870–2877. (b) Broderick, E. M.; Guo, N.; Vogel, C. S.; Xu, C.; Sutter, J. T.; Miller, J. T.; Meyer, K.; Mehrkhodavandi, P.; Diaconescu, P. L. *J. Am. Chem. Soc.* **2011**, *133* (24), 9278–9281.
- (6) (a) Cadierno, V.; Diez, J.; Garcia-Alvarez, J.; Gimeno, J. *Chem. Commun.* **2004**, *16*, 1820–1821. (b) Cavell, R. G.; Kamalesh Babu, R. P.; Aparna, K. *J. Organomet. Chem.* **2001**, *617*–618, 158–169. (c) Cooper, O. J.; McMaster, J.; Lewis, W.; Blake, A. J.; Liddle, S. T. *Dalton Trans.* **2010**, *39* (21), 5074–5076. (d) Hill, M. S.; Hitchcock, P. B. *Polyhedron* **2007**, *26* (6), 1245–1250. (e) Johnson, K. R. D.; Hayes, P. G. *Organometallics* **2009**, *28* (21), 6352–6361. (f) Lin, G.; Jones, N. D.; Gossage, R. A.; McDonald, R.; Cavell, R. G. *Angew. Chem., Int. Ed.* **2003**, *42* (34), 4054–4057. (g) Oulié, P.; Freund, C.; Saffon, N.; Martin-Vaca, B.; Maron, L.; Bourissou, D. *Organometallics* **2007**, *26* (27), 6793–6804. (h) Panda, T. K.; Roesky, P. W. *Chem. Soc. Rev.* **2009**, *38* (9), 2782–2804. (i) Ruther, T.; Cavell, K. J.; Braussaud, N. C.; Skelton, B. W.; White, A. H. *J. Chem. Soc., Dalton Trans.* **2002**, *24*, 4684–4693.
- (7) (a) Buchard, A.; Auffrant, A.; Ricard, L.; Le Goff, X. F.; Platel, R. H.; Williams, C. K. *Dalton Trans.* **2009**, *46*, 10219–10222. (b) Buchard, A.; Platel, R. H.; Auffrant, A.; Le Goff, X. F.; Le Floch, P.; Williams, C. K. *Organometallics* **2010**, *29* (13), 2892–2900.
- (8) Cao, T.-P.-A.; Labouille, S.; Auffrant, A.; Jean, Y.; Le Goff, X. F.; Le Floch, P. *Dalton Trans.* **2011**, ASAP, DOI:10.1039/C1DT10906E.
- (9) (a) Ragauskas, A. J.; Williams, C. K.; Davison, B. H.; Britovsek, G.; Cairney, J.; Eckert, C. A.; Frederick, W. J.; Hallett, J. P.; Leak, D. J.; Liotta, C. L.; Mielenz, J. R.; Murphy, R.; Templer, R.; Tschaplinski, T. *Science* **2006**, *311* (5760), 484–489. (b) Williams, C. K.; Hillmyer, M. A. *Polym. Rev.* **2008**, *48* (1), 1–10. (c) Dove, A. P. *Chem. Commun.* **2008**, *48*, 6446–6470. (d) Platel, R. H.; Hodgson, L. M.; Williams, C. K. *Polym. Rev.* **2008**, *48* (1), 11–63. (e) Inkinen, S.; Hakkarainen, M.; Albertsson, A. C.; Sodergard, A. *Biomacromolecules* **2011**, *12* (3), 523–532.
- (10) (a) Dechy-Cabaret, O.; Martin-Vaca, B.; Bourissou, D. *Chem. Rev.* **2004**, *104*, 6147–6176. (b) Ajellal, N.; Carpentier, J. F.; Guillaume, C.; Guillaume, S. M.; Helou, M.; Poirier, V.; Sarazin, Y.; Trifonov, A. *Dalton Trans.* **2010**, *39* (36), 8363–8376.
- (11) (a) Gross, R. A.; Kumar, A.; Kalra, B. *Chem. Rev.* **2001**, *101* (7), 2097–2124. (b) Kamber, N. E.; Jeong, W.; Waymouth, R. M.; Pratt, R. C.; Lohmeijer, B. G. G.; Hedrick, J. L. *Chem. Rev.* **2007**, *107* (12), 5813–5840.
- (12) (a) Bouyahy, M.; Ajellal, N.; Kirillov, E.; Thomas, C. M.; Carpentier, J. F. *Chem.—Eur. J.* **2011**, *17* (6), 1872–1883. (b) Nie, K.; Gu, X. Y.; Yao, Y. M.; Zhang, Y.; Shen, Q. *Dalton Trans.* **2010**, *39* (29), 6832–6840. (c) Clark, L.; Cushion, M. G.; Dyer, H. E.; Schwarz, A. D.; Duchateau, R.; Mountford, P. *Chem. Commun.* **2010**, *46* (2), 273–275. (d) Zhang, Z. J.; Xu, X. P.; Li, W. Y.; Yao, Y. M.; Zhang, Y.; Shen, Q.; Luo, Y. *J. Inorg. Chem.* **2009**, *48* (13), 5715–5724. (e) Dyer, H. E.; Huijser, S.; Schwarz, A. D.; Wang, C.; Duchateau, R.; Mountford, P. *Dalton Trans.* **2008**, *1*, 32–35. (f) Amgoune, A.; Thomas, C. M.; Roisnel, T.; Carpentier, J. F. *Chem.—Eur. J.* **2006**, *12*, 169–179. (g) Bonnet, F.; Cowley, A. R.; Mountford, P. *Inorg. Chem.* **2005**, *44* (24), 9046–9055. (h) Cai, C. X.; Amgoune, A.; Lehmann, C. W.; Carpentier, J. F. *Chem. Commun.* **2004**, 330–331. (i) Platel, R. H.; White, A. J. P.; Williams, C. K. *Inorg. Chem.* **2008**, *47* (15), 6840–6849. (j) Platel, R. H.; White, A. J. P.; Williams, C. K. *Chem. Commun.* **2009**, *27*, 4115–4117. (k) Hodgson, L. M.; Platel, R. H.; White, A. J. P.; Williams, C. K. *Macromolecules* **2008**, *41* (22), 8603–8607. (l) Platel, R. H.; Hodgson, L. M.; White, A. J. P.; Williams, C. K. *Organometallics* **2007**, *26* (20), 4955–4963. (m) Hodgson, L. M.;

- White, A. J. P.; Williams, C. K. *J. Polym. Sci., Part A: Polym. Chem.* **2006**, *44* (22), 6646–6651. (n) Buffet, J.-C.; Kapelski, A.; Okuda, J. *Macromolecules* **2010**, *43* (24), 10201–10203. (o) Mahrova, T. V.; Fukin, G. K.; Cherkasov, A. V.; Trifonov, A. A.; Ajellal, N.; Carpentier, J. F. *Inorg. Chem.* **2009**, *48* (9), 4258–4266. (p) Broomfield, L. M.; Wright, J. A.; Bochmann, M. *Dalton Trans.* **2009**, 39, 8269–8279. (q) Alaaeddine, A.; Thomas, C. M.; Roisnel, T.; Carpentier, J. F. *Organometallics* **2009**, *28* (5), 1469–1475. (r) Broderick, E. M.; Diaconescu, P. L. *Inorg. Chem.* **2009**, *48* (11), 4701–4706. (s) Ma, H.; Spaniol, T. P.; Okuda, J. *Inorg. Chem.* **2008**, *47* (8), 3328–3339. (t) Ma, H. Y.; Spaniol, T. P.; Okuda, J. *Angew. Chem., Int. Ed.* **2006**, *45* (46), 7818–7821. (u) Ma, H.; Okuda, J. *Macromolecules* **2005**, *38*, 2665–2673. (v) Grunova, E.; Kirillov, E.; Roisnel, T.; Carpentier, J. F. *Organometallics* **2008**, *27* (21), 5691–5698. (w) Arnold, P. L.; Buffet, J. C.; Blaudeck, R. P.; Sujecki, S.; Blake, A. J.; Wilson, C. *Angew. Chem., Int. Ed.* **2008**, *47* (32), 6033–6036. (x) Arnold, P. L.; Buffet, J. C.; Blaudeck, R.; Sujecki, S.; Wilson, C. *Chem.—Eur. J.* **2009**, *15* (33), 8241–8250. (y) Ajellal, N.; Lyubov, D. M.; Sinenkov, M. A.; Fukin, G. K.; Cherkasov, A. V.; Thomas, C. M.; Carpentier, J. F.; Trifonov, A. A. *Chem.—Eur. J.* **2008**, *14* (18), 5440–5448. (z) Heck, R.; Schulz, E.; Collin, J.; Carpentier, J. F. *J. Mol. Catal. A: Chem.* **2007**, *268* (1–2), 163–168. (aa) Westmoreland, I.; Arnold, J. *Dalton Trans.* **2006**, 4155. (ab) Patel, D.; Liddle, S. T.; Mungur, S. A.; Rodden, M.; Blake, A. J.; Arnold, P. L. *Chem. Commun.* **2006**, 10, 1124–1126. (ac) Alaaeddine, A.; Amgoune, A.; Thomas, C. M.; Dagorne, S.; Bellemin-Lapponnaz, S.; Carpentier, J.-F. *Eur. J. Inorg. Chem.* **2006**, 3652–3658. (ad) Ovitt, T. M.; Coates, G. W. *J. Am. Chem. Soc.* **2002**, *124*, 1316. (ae) Aubrecht, K. B.; Chang, K.; Hillmyer, M. A.; Tolman, W. B. *J. Polym. Sci., Part A: Polym. Chem.* **2001**, *39*, 284–293. (af) Chamberlain, B. M.; Sun, Y.; Hagadorn, J. R.; Hemmesch, E. W.; Young, V. G. Jr.; Pink, M.; Hillmyer, M. A.; Tolman, W. B. *Macromolecules* **1999**, *32* (7), 2400–2402. (ag) Simic, V.; Girardon, V.; Spassky, N.; Hubert-Pfalzgraf, L. G.; Duda, A. *Polym. Degrad. Stab.* **1998**, *59*, 227–229. (ah) Simic, V.; Spassky, N.; Hubert-Pfalzgraf, L. G. *Macromolecules* **1997**, *30*, 7338–7340. (ai) Stevels, W. M.; Ankone, M. J. K.; Dijkstra, P. J.; Feijen, J. *Macromolecules* **1996**, *29*, 6132–6138.
- (13) (a) Shang, X. M.; Liu, X. L.; Cui, D. M. *J. Polym. Sci., Part A: Polym. Chem.* **2007**, *45* (23), 5662–5672. (b) Miao, W.; Li, S. H.; Zhang, H. X.; Cui, D.; Wang, Y. R.; Huang, B. T. *J. Organomet. Chem.* **2007**, *692* (22), 4828–4834. (c) Liu, X. L.; Shang, X. M.; Tang, T.; Hu, N. H.; Pei, F. K.; Cui, D. M.; Chen, X. S.; Jing, X. B. *Organometallics* **2007**, *26* (10), 2747–2757. (d) Amgoune, A.; Thomas, C. M.; Carpentier, J. F. *Pure Appl. Chem.* **2007**, *79* (11), 2013–2030. (e) Amgoune, A.; Thomas, C. M.; Carpentier, J. F. *Macromol. Rapid Commun.* **2007**, *28* (6), 693–697. (f) Zhao, W.; Cui, D. M.; Liu, X. L.; Chen, X. S. *Macromolecules* **2010**, *43* (16), 6678–6684.
- (14) Hillesheim, N. S.; Elfferding, M.; Linder, T.; Sundermeyer, J. Z. *Anorg. Allg. Chem.* **2010**, *636* (9–10), 1776–1782.
- (15) Coudane, J.; Ustariz-Peyret, C.; Schwach, G.; Vert, M. *J. Polym. Sci., Part A: Polym. Chem.* **1997**, *35*, 1651–1658.
- (16) Wu, J. C.; Huang, B. H.; Hsueh, M. L.; Lai, S. L.; Lin, C. C. *Polymer* **2005**, *46* (23), 9784–9792.
- (17) Chen, H.-Y.; Huang, B.-H.; Lin, C.-C. *Macromolecules* **2005**, *38* (13), 5400–5405.
- (18) Binda, P. I.; Delbridge, E. E. *Dalton Trans.* **2007**, *41*, 4685–4692.
- (19) Williams, C. K.; Breyfogle, L. E.; Choi, S. K.; Nam, W.; Young, V. G.; Hillmyer, M. A.; Tolman, W. B. *J. Am. Chem. Soc.* **2003**, *125* (37), 11350–11359.
- (20) Zell, M. T.; Padden, B. E.; Paterick, A. J.; Thakur, K. A. M.; Kean, R. T.; Hillmyer, M. A.; Munson, E. J. *Macromolecules* **2002**, *35* (20), 7700–7707.
- (21) (a) Chmura, A. J.; Davidson, M. G.; Frankis, C. J.; Jones, M. D.; Lunn, M. D. *Chem. Commun.* **2008**, *11*, 1293–1295. (b) Liu, X.; Shang, X.; Tang, T.; Hu, N.; Pei, F.; Cui, D.; Chen, X.; Jing, X. *Organometallics* **2007**, *26* (10), 2747–2757. (c) Chisholm, M. H.; Gallucci, J.; Phomphrai, K. *Chem. Commun.* **2003**, *1*, 48–49.
- (22) Kocher, N.; Leusser, D.; Murso, A.; Stalke, D. *Chem.—Eur. J.* **2004**, *10* (15), 3622–3631.
- (23) Stridsberg, K.; Stridsberg, K. M. *Adv. Polym. Sci.* **2002**, *157* (Degradable), 41–65.
- (24) Sobota, P.; Utko, J.; Szafert, S. *Inorg. Chem.* **1994**, *33* (23), 5203–5206.
- (25) Bianchi, A.; Bernardi, A. *J. Org. Chem.* **2006**, *71* (12), 4565–4577.
- (26) Dorgan, J. R.; Janzen, J.; Knauss, D. M.; Hait, S. B.; Limoges, B. R.; Hutchinson, M. H. *J. Polym. Sci., Part B: Polym. Phys.* **2005**, *43* (21), 3100–3111.
- (27) Altomare, A.; Burla, M. C.; Camalli, M.; Cascarano, G. L.; Giacovazzo, C.; Guagliardi, A.; Moliterni, A. G. G.; Polidori, G.; Spagna, R. *J. Appl. Crystallogr.* **1999**, *32*, 115–119.
- (28) Sheldrick, G. M. *SHELXL-97*; Universität Göttingen: Göttingen, Germany, 1997.
- (29) Farrugia, L. J. Department of Chemistry, University of Glasgow, 2001.